GEOCHEMISTRY AND ALTERATION MAPPING OF THE PABOASE DEPOSIT AT CHIRANO GOLD MINES, GHANA

BY

ARNOLD BALER AFLOE

(10362386)

This dissertation is submitted to the University of Ghana, Legon in partial fulfillment of the requirement for the award of MSc Mineral Exploration degree

Department of Earth Science

University of Ghana, Legon

June 2014

DECLARATION

This research project was submitted as part of a postgraduate Masters Project in Mineral Exploration at the University of Ghana. I hereby declare that the work in this dissertation is original and has not been submitted anywhere for the award a degree. Works from other authors used have been duly acknowledged. The project was undertaken under the supervision of Dr. Johnson Manu.

Date: June, 2014

.....

ARNOLD BALER AFLOE
(Student)

.....

DR. JOHNSON MANU
(Supervisor)

ABSTRACT

The Paboase deposit located in the Chirano gold district is hosted in Paleoproterozoic rocks within the Sefwi-Bibiani volcanic belt of the Birimian, which has been regionally metamorphosed to greenschist facies. Gold mineralization at Paboase is largely hosted by albite-pyrite-carbonate altered mafic and porphyry intrusive rocks rather than Birimian sedimentary rocks and graphitic shear zones which are well known style of mineralization in southwest Ghana. Multi-element geochemistry shows a quite weak fractionation trend among the mafic rocks, despite the doleritic and gabbroic textures. One different exotic mafic dyke signature can be recognised. Amongst the porphyries, two different compositional groups were recognized. There is a small scale intermixing of felsic dykes within mafic volcanics.The dominant alteration signature is intense albitisation along with ferroan dolomite and pyrite. There is about 150 m wide zone where the Analytical Spectral Device (ASD) maps strong carbonate alteration. The proximal alteration is carbobonate-albite-pyrite. This is surrounded by a distal halo of sericite-chlorite. Within the porphyries, the mineralogy is sericite-rich. Sericite-chlorite alteration is very widespread in the mafic rocks. Paboase has a Tungsten-Molybdenum-Bismuth-Terrarium (W-Mo-Bi-Te) signature. The Mo, Bi and Te have a strongly skewed distribution, and they are highly correlated with gold, so their usefulness as pathfinders is limited. The tungsten is remarkably uniformly distributed in the albite-dolomite rocks, and has a halo extending far beyond the footprint of the gold. Tungsten is therefore the best pathfinder for gold at Paboase. The host rocks for the anomalous W are essentially just albite-pyrite-dolomite rocks. Arsenic is clearly depleted in the proximal parts of the system compared to the pelitic sedimentary hosted graphitic shear zones of the Ashanti and Bogoso deposits in Ghana. It is suggested that the depletion of arsenic is as a result of flushing the rocks with an oxidized fluid early in the history of the system.

DEDICATION

This work is dedicated to the Lord Jesus Christ for bringing me to this beautiful unexpected end.

ACKNOWLEDGEMENT

This project was sponsored by Kinross Chirano Gold Mines Ltd. and the support of the Exploration Department in carrying out the project is greatly acknowledged. I wish to express my heart felt gratitude to the Kinross Director of Exploration for Africa, Dr Zak Sanfo and all the Exploration team members for their support throughout the project duration.

My deeply felt gratitude also goes to my supervisor, Dr Johnson Manu of the University of Ghana for his leadership, expertise and scrutiny that has influenced the success of the work. This project has also benefitted greatly from Dr Scott Halley of Mineral Mapping Proprietary (Pty) Limited, Australia.

CONTENTS

LIST OF FIGURES

LIST OF TABLES

CHAPTER ONE

INTRODUCTION

1.1 Background

The Chirano Mine lies within the Paleoproterozoic terrain of southwest Ghana. It is located along the margin of the Sefwi-Bibiani Belt adjacent to the Kumasi Basin to the east. Both the Sefwi-Bibiani Belt and the Kumasi Basin comprise rocks of Birimian age, with the belt dominated by mafic volcanic rocks and the basin typified by fine grained, deep water sediments. Both are intruded by granites (Fig. 1.1).

The structurally controlled deposit mine which had its first gold pour in 2005 is 100% owned by Kinross, a Canadian based Company and is operating under the subsidiary name Chirano Gold Mines Limited (CGML). Kinross acquired the mine from Red Back Mining Incorporation in September 17, 2010. The Chirano Gold district lies along a 10km strike in Southwest Ghana approximately 130km Southwest of Kumasi, the second largest city of Ghana. The current mining operation consists of ten open pits and two underground deposits. Eight have been already mined out and closed down.

Exploration at Chirano has identified a series of deposits scattered along the mineralised shear zone which currently extends for ~10km. This structure coincides with parts of the Chirano Shear Zone and one or more related splays which form part of a prominent fault zone that includes the Bibiani Shear Zone and other related thrust faults. The deposits have been subjected to ground geophysics, geological mapping and on-going drilling activities to define reserves and resources. Currently exploration focuses on the discovery of new deposits along the mine trend and district targets and high grade shoots below the existing pits.

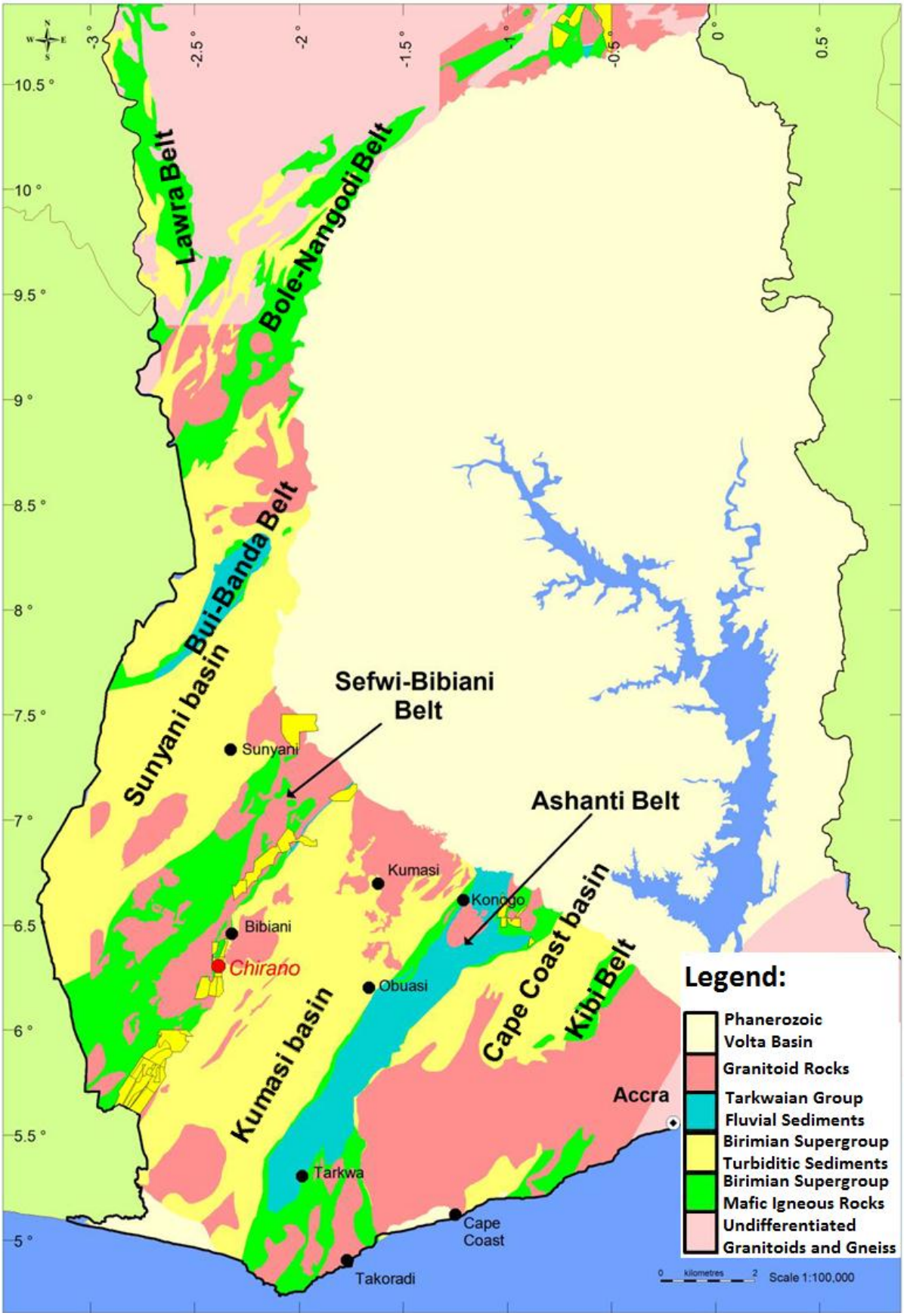

Fig. 1.1 Map of Ghana showing the location of Chirano Gold Mines and the various gold belts.

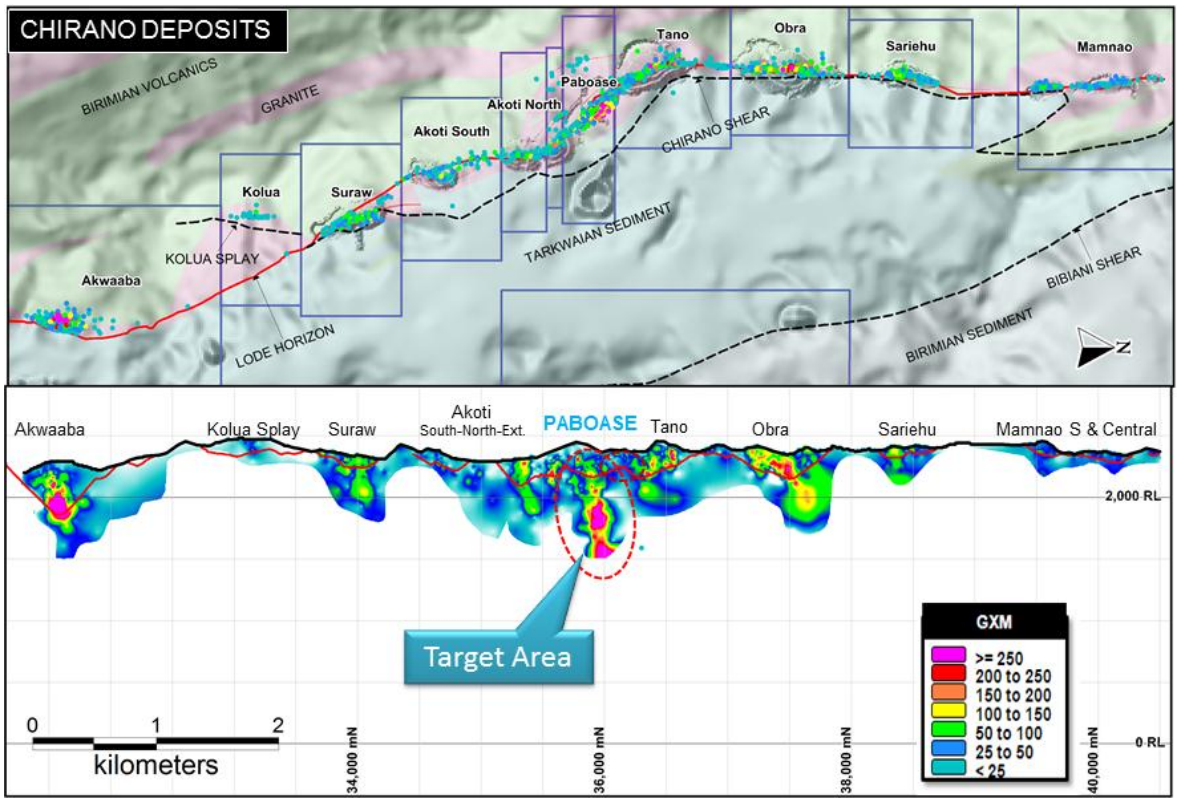

Fig. 1.2 The Chirano deposits along the mineralized shear zone.

1.2 Problem Statement

The Chirano deposits were discovered using geological mapping and soil geochemistry which were followed by drilling. Drill hole information from various geologists was used to define the resources and reserves database. However, this logged information from different geologists could be very subjective especially when logging drill chips. The present deposits are being mined out and there is the need to discover new ones to extend the mine life. Therefore current exploration activities are focused on the discovery of new deposits along the mine trend and district targets as well as high grade shoots below the existing pits. Due to the inconsistencies in the logged data over the years, it has been very difficult to determine the actual host rock and the proximal and distal alterations that can be used to improve exploration successes along the mine trend and district targets. In addition, little is known about the pathfinder's signature of the deposits.

1.3 Scope and Objectives

This project aims broadly at using Analytical Spectra Devices (ASD) TerraSpec Short Wave Infrared (SWIR) alteration data and rock multi-element geochemistry to determine the alteration signature, host rock lithology and pathfinders of the ore system. Among the specific objectives are to;

- distinguish the host rock within the intensely deformed and altered package,
- identify the alteration mineralogy both proximal and distal and
- identify the pathfinder element signature of the ore system.

1.4 Justification

Gold deposits are hard to find, but the hydrothermal systems that host gold have much larger footprints. Pathfinder minerals and alteration haloes can be used to first identify where the hydrothermal systems are, and then narrow down to the alteration cells to find the gold. In the quest to find new gold deposits both on the extensively explored and less explored areas of the properties on the Sefwi belt and also to increase the reserves for the existing ones, there is the need to improve the knowledge of the host rock geology and the distal and proximal alteration signatures to enhance drilling targeting. In addition, a good knowledge about the pathfinder minerals can help improve exploration successes on properties along the belt. Knowing and modelling the alteration halo of the mineralized domain could also be used as grade boundary checks for resource evaluation in the absence of a good geological model for the deposit.

The ASD terraspec has proven to be a very fast and systematic logging tool as it removes geologist's bias from alteration logging and hence generates a consistent alteration data that can be used to determine the proximal and distal alteration.

CHAPTER TWO

LITERATURE REVIEW

2.1 Regional Geology

The study area is within the Paleoproterozoic terrain of Southwest Ghana. Paleoproterozoic supracrustal rocks in southwest Ghana are subdivided into two main groups; the volcanic-sedimentary Birimian Supergroup and the overlying clastic sedimentary rocks of the Tarkwaian Group. These paleoproterozoic rocks have been subjected to two main orogenic cycles between ~2250 and 2088 Ma, the progressive Eburnean orogeny, also referred to as the Eburnean 1 and 2 orogenies (Allibone et al., 2002).

The Birimian successions comprises of sedimentary/volcaniclastic lithologies which consist of primarily mafic rocks erupted and emplaced during the Eburnean orogenic cycle, such as tholeiitic basalts and lesser calc-alkaline and rhyolitic volcanics (Lower Birimian). It is thought that these rocks make up the basement of the younger Birimian turbiditic fluvial and sedimentary rocks and metamorphic equivalents such as phyllites and argillites, forming the sedimentary basins in the region (Allibone et al. 2004).These constitute five northeast-trending volcanic belts (Upper Birimian). Collectively the volcanics and sediments described above are known as the Birimian Supergroup (Fig.1.1). Available field evidence suggests that the volcanic and sedimentary rocks are lateral equivalents (Leube et al. 1990).

The Tarkwaian system is dominated by coarse clastic sedimentary rocks of fluvio-deltaic origin, sandstones, conglomerates, quartzites and other metamorphic equivalents such as phyllites and argillites. Allibone et al. (2004) note that deposition of this group of sedimentary rocks occurred coincidentally with initial deformation of the Birimian Supergroup early in the Eburnean 2 orogeny but prior to granitoid emplacement. Generally

the Tarkwaian Group sediments are confined to the mafic igneous belts associated with the Birimian Supergroup, usually occurring either in unconformable stratigraphic contact or as imbricated fault-bounded slices.

2.1.1 Regional Scale Metamorphism

Defining the prominent structural fabric in southwest Ghana and the boundaries between the volcanic belts and sedimentary basins are numerous major thrust faults, progressive folding and a late phase of localised strike-slip shearing (Eisenlohr and Hirdes, 1992; Allibone et al., 2002). These formed as the result of northwest – southeast directed crustal shortening (Oberthür et al., 1996; Allibone et al., 2004). Examples of both high and low strain periods of deformation are recorded by this event. Low strain deformation includes rocks locally containing a regionally penetrative S_1 foliation, sub-parallel to bedding. High strain regions commonly occur at the northwest margins of the volcanic belts, with thrusts and shears of high strain zones displaying an S_2 foliation. However, regions of least strain display volcano-sedimentary rocks that are generally unfoliated.

Birimian and Tarkwaian rocks were deformed and metamorphosed under greenschist facies conditions during the Eburnean tectonothernal event at ca. 2.1 Ga (Oberthur et al., 1998). However, petrographic and mineral-chemical investigations of mineral assemblages carried out by Yao and Robb (2000) on metamorphosed volcanics and granitoids of the Ashanti belt suggest peak metamorphic conditions were higher. From this information, it was concluded that metamorphic conditions of Birimian rocks reached amphibolite facies at temperatures ~500-650°C and pressures of 5-6 kbar. It is therefore possible that either, greenschist facies conditions are the result of retrograde metamorphism near to the end of the orogeny after any exhumation of mid-crustal rocks, or metamorphic grade varied on a regional scale.

2.1.2 Intrusive Events

Two main intrusive periods have affected the Birimian rocks of southwest Ghana and these are the Cape Coast and Dixcove type granitoids as originally mapped and recorded (Taylor et al., 1992; Oberthür et al., 1996, 1998; Yao et al., 2001). More recently Cape Coast and Dixcove have been reclassified as belt and basin type granitoids respectively, although further debate exists as to which type is belt or basin and the basic geochronology of the granitoids (Taylor et al., 1992; Oberthür et al., 1996; Yao et al., 2001).

Taylor et al., (1992) and Oberthür et al., (1996) state that the original Cape Coast granitoid has been reclassified as basin type, which are S-type granitoids that are locally migmatitic. This is contrasted by Yao et al., (2001) who reclassify the Cape Coast granitoids as I-type belt granitoids. Since this is the most recent classification scheme it is the scheme that will be utilised throughout the remainder of this report.

The belt type granitoids are older than the basin type by approximately 90-10 m.y. (Yao et al. 2001). Granitoids within the volcanic belts are typically tonalitic to granodioritic in composition with a metaluminous character containing hornblende. They occur along the volcanic belts as small to medium sized plutonic bodies as I-type granitoids formed by partial melting of basaltic rocks (Yao et al., 2001; Taylor et al., 1992).

By contrast, the basin type granitoids are peraluminous containing biotite with very little hornblende observed. Basin type granitoids are emplaced as large batholiths into basin sediments and are considered to have formed from minimum melting of crustal materials with a minor mantle component (Yao et al., 2001). Taylor et al. (1992) propose a theory that basin type granitoids may represent an old continental basement that the Birimian

supracrustals were deposited onto, however it is clear from field observations that the granitoids are intrusive in nature.

2.2 Local Geology

The Chirano gold deposits are hosted near the boundary of Birimian mafic igneous rocks with Tarkwaian sedimentary rocks. Where faulted, this boundary has been intruded by tonalite. Volcano-sedimentary rocks and the tonalites are metamorphosed to greenschist facies assemblages and in least strained regions are generally unfoliated (Allibone et al., 2004). Previously, it was considered that tonalite intrusions were the main host to gold mineralisation (Allibone et al., 2004). However, recent exposures in open-pits have shown that the volume of tonalite has been over-estimated at several deposits, which are mostly hosted within strongly hydrothermally altered mafic igneous rocks.

Basaltic and doleritic rocks, with subordinate gabbro, tonalite and diorite intrusions of the Sefwi-Bibiani volcanic belt dominate the western domain. The central domain is composed mainly of Tarkwaian Group rocks of siltstone, sandstone, grit and conglomerates with minor basaltic and doleritic rocks. Birimian sedimentary rocks made up of turbiditic graywackes, siltstones and minor fine grained sandstones on the western margin of the Kumasi basin comprise the eastern domain (Allibone et al., 2004). Between the western and central domains is the Chirano Shear Zone (CSZ) that varies in width along strike, with the larger graphitic and chloritic Bibiani shear zone separating the central and eastern domains. The 4 Million ounces Bibiani gold deposit lies on the intersection of these two shear zones north of the Chirano gold district.

2.2.1 Deformational Events and Structures

Two deformation events are recognised and it is likely that beyond these at least two more deformation events might have occurred (Table 2.1) but this in all probability represents one main progressive period of deformation rather than 4 distinctly separate events.

The first deformation event (D_1), which is speculative, involved thrusting and repetition of Birimian and Tarkwaian rocks. The second phase of deformation (D_2), which is observed in the field, comprises open, gently north and south plunging folds. The folds are recognised by bedding-cleavage relationships within the Tarkwaian sedimentary rocks. It is likely that folding involved the Birimian rocks similar to other parts of SW Ghana. Steeply-dipping, North to NW-striking fault zones formed during (D_3). The mineralised (D_3) 'fault zone' at Chirano is referred to as the Chirano Shear Zone (CSZ) which occurs over a length of 10km locally, but exhibits a much longer strike length north and south away from the near mine area (SRK, 2008).

Early tonalite intrusions along the CSZ were followed by later hydrothermal alteration and gold mineralisation. It is possible that (D_2) folds are related to shearing on the CSZ and hence do not represent a different deformation event. Generally it is thought that it is a local deformation sequence within which folding and faulting occurred as different events. Further work on the spatial distribution of the folds may elucidate the relationship between folding and faulting. A fourth phase of deformation (D_4) involving NE-striking faults crosscutting (D_3) shear zones, for example the CSZ, is speculated (SRK, 2008).

Table 2.1 Structural evolution of the Chirano Gold District (SRK, 2008).

	Structural Event	Magmatic Event	Metamorphic-Hydrothermal Event
D_4?	NE-striking faults		
D_3	Subvertical N-striking shear zones (Chirano Shear Zone)		Gold mineralisation
		Granitoids (tonalite intrusions)	
D_2	Gently N-and S-plunging folds		
D_1?	Thrusting		

All of the deposits within the Chirano gold district are located within or along a zone of strain that flanks the CSZ to the west within a zone of altered and deformed rocks known as the Chirano Lode Horizon (Allibone et al., 2004). There is anomalous gold along the Chirano Lode Horizon at length and depth, it also contains structures varying in size through foliation and veining to small faults.

The protolith of the CSZ is difficult to identify given that much of the primary mineralogy and textures have been obscured by hydrothermal alteration, faulting and thrusting (SRK, 2008). This is most apparent in the ore zones, where such processes were more intense. Of the numerous structural controls on gold mineralisation, the CSZ is the main district-scale control. However within the deposits, mineralisation and orientation of high-grade shoots is controlled by local host rocks and structural features such as splay faults off the main shear zone and dip jogs.

The CSZ is the principal deformation corridor along which numerous structural, magmatic and metamorphic processes occurred during the Eburnian orogeny. The CSZ initially experienced large-scale regional thrusting formed by NW-SE compression, and then a later transpressional strike-slip event that formed a sinistral through-going fault system. It is this

strike-slip system that produced a regional relay zone containing a related series of dilational jogs (pull-apart basins with normal faults, veining and breccias) and contractional jogs/restraining bends (areas of crustal shortening, local uplift, reverse faulting and folding) (SRK, 2008).

There is evidence that the Chirano structural corridor, or fault zone was active over an extended period of geologic time (~164 Ma between 2,250 Ma and 2,086 Ma, Allibone et al, 2004), and was therefore the locus of several tectonic, magmatic and hydrothermal events. Gold mineralization was probably one of the last events to take place within this tectonic corridor.

Some of the deposits at Chirano may have formed close to the ductile to semi-brittle level in the crust as they commonly show evidence that regional scale ductile forces (high temperature and pressure) were at play during strike-slip movement. For example, at Akoti a central zone of intense foliation and mylonite rock takes a ~40° swing from a northeast strike to a northern strike in less than 50 metres length. The rock appears to bend and has suffered very little brittle deformation immediately along this zone (SRK, 2008).

2.2.2 Hydrothermal Alterations

Intense hydrothermal alteration can be seen at the Chirano deposits following the regional greenschist facies metamorphism. At Chirano there are two main zones/periods of hydrothermal alteration as observed and logged by geologists, the first of which consists of albite, quartz, pyrite, hematite, rutile +/- leucoxene and gold. This alteration is especially prevalent surrounding the tonalite intrusives and occurs as a broader alteration halo in

comparison to the later carbonate alteration within the mineralized zone (Allibone et al., 2004).

Graphite is present as a silvery black infill intergrown with volumetrically significant sulphides along stylolitic breccia surfaces, as well as inclusions in silica-albite-pyrite breccia fill, in zones of strongly elevated gold mineralization. Graphite has not been observed outside the mineralized domain in the immediate Pabaose area. It has been observed (Beeson, 2011) that the graphite has been introduced directly into the mineralized domain from somewhere else through fluid flow. Furthermore, the intimate association between graphite, pyrite deposition and gold mineralization provides compelling evidence that introduction of graphite was directly related to gold mineralization. Graphite formation suggests that reduced carbon has been forced into the mineralized domain (probably through a methane-rich fluid/gas). The source of this fluid is yet to be fully determined, but there is a good chance that graphitic sedimentary rocks of the Kumasi Basin have provided this fluid. Graphitic phyllite and shale of the Kumai Basin has been encountered within 2km east of Paboase and significant grid-NW striking faults are known to connect Paboase with this basinal sequence (Beeson, 2011).

A gold prospect in Ekyuabo which occurs in the Kumasi basin sequence in Chirano through drilling has revealed a system of graphite-enriched faults in the phyllite and shale suggesting that carbon was mobilized during faulting. It seems quite likely then that carbon (as methane) was mobilized out of the Kumasi Basin sequence during basin inversion and injected through cross-cutting fault networks into structures like the Paboase shear-breccia system during porphyry injection. The deposit has a pyrite-arsenopyrite-graphite association along with intense sericite and an As-Sb pathfinder signature (Halley, 2011).

2.2.3 Gold mineralisation at Chirano

Gold mineralisation within the deposits is strongly associated with structural aspects including small splay faults from the main CSZ as well as veins and foliations. Dip jogs and dilational sites along the CSZ are found to be the areas of most economic mineralisation due to the greater amount of tonalite intrusions leading to broader zones of hydrothermal alteration (SRK, 2008). The gold mineralisation is associated with pyrite and is generally very fine grained with only one or two occurrences of visible gold in drill core. Even in polished sections of very high grade pyrite concentrates relatively few gold grains are seen, consequently much of the gold appears to be microscopic.

Carbonate altered rocks commonly have gold grades up to 5g/t and locally as high as 10+g/t. Grades higher than approximately 3g/t generally occur in more intensely altered zones that lack primary texture and where the amount of disseminated pyrite and/or the density of the infilling of quartz ± carbonate ± pyrite ± Au veinlets is greater.Gold, Ag-Au telluride, galena, tetrahedrite, bornite and chalcopyrite occur as inclusions in pyrite and less commonly as isolated grains within the matrix of the carbonate alteration (Allibone et al., 2004).

2.3 The Paboase Deposit

The Paboase deposit (Fig. 1.2) was discovered initially as an open pit resource. Further deep drilling below the pit has resulted in the discovery of the underground resource which was the second underground to be discovered after Akwaaba. The Akwaaba deposit is the southernmost in the Chirano gold district and was the first to have underground resources exploited. The deposit consists of relatively moderate to high grade gold mineralization in comparison with some of the northern deposits along the Chirano system. The Paboase open

pit has been closed as of the time of this project whiles the underground reserve was at its advance development stage.

It is situated about 350 m west of the Chirano Shear Zone and changes strike from north east at its southern extent and bend to north west across the main orebody before returning to its original trend at the base of the Tano deposit. On a regional scale this change in strike possibly represents a releasing bend allowing for increased gold mineralization (Beeson, 2011) (Fig. 2.1).

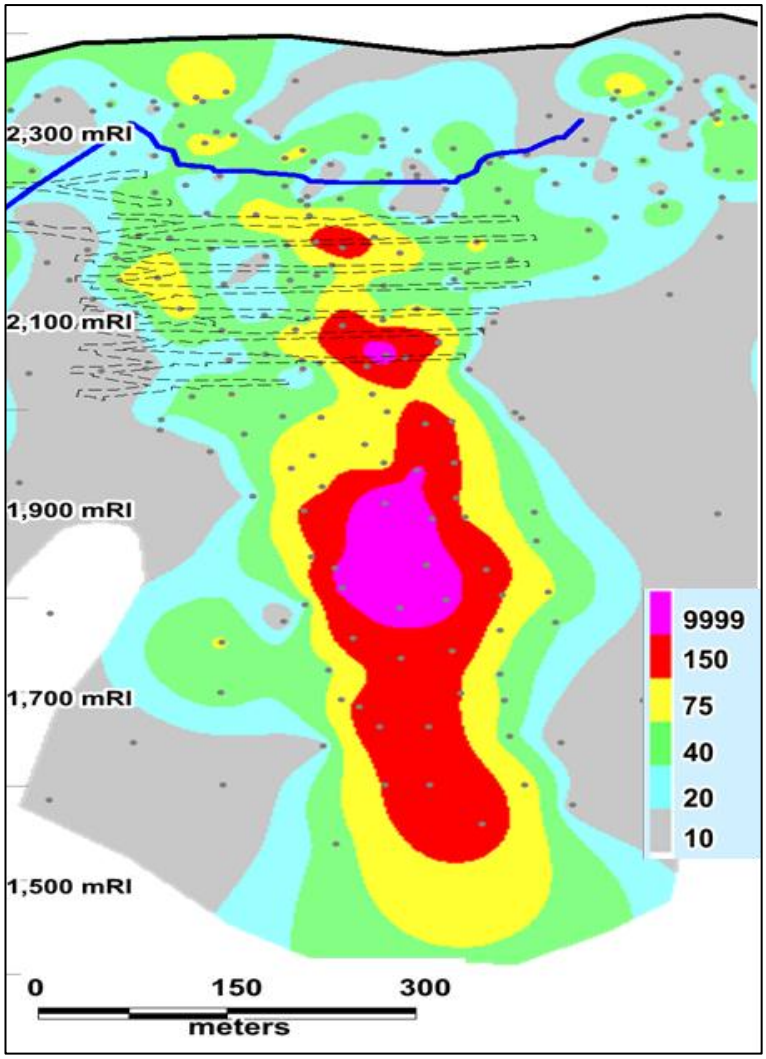

Fig. 2.1 True width gram metre longitudinal section of the Paboase deposit (looking west).

2.3.1 Geology and Structures

The Paboase mineralized zone show various structural features ranging from ductile to brittle-ductile foliations and shears, to brittle structures including breccias, veins, fault zones and fractures. On a volume basis the sequence does not appear to be highly deformed; strain (particularly ductile to brittle-ductile strain) is strongly partitioned into particular parts of the rock sequence. In addition, there is a noticeable asymmetry in deformation intensity and style from hanging wall (east) to footwall (west). Ductile to brittle-ductile structures evident at Paboase comprise penetratively-foliated zones varying from a few centimetres wide to several meters wide down-hole. These foliated zones represent discrete domains of shearing with symmetric to locally asymmetric internal fabrics (Beeson, 2011) (Fig. 2.2).

Fig. 2.2 Brittle-ductile shear-breccia zone fabric located west of the mineralized zone at Paboase (low or no Au grade) (Beeson, 2011).

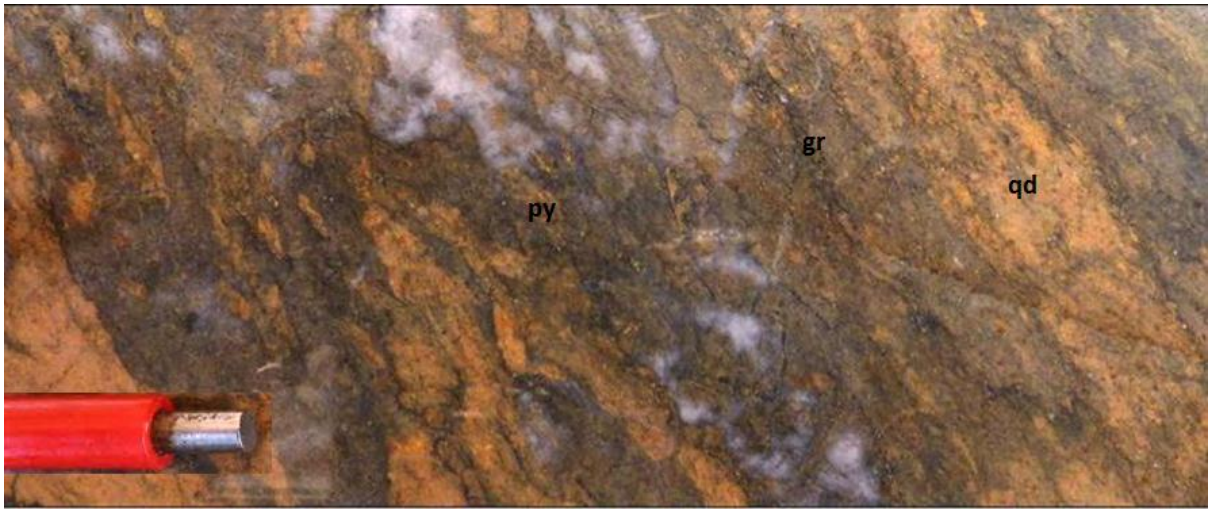

Fig. 2.3 Brittle-ductile fabric overprinting ankerite-albite-silica-pyrite (py)-graphite (gr) breccia fabric in quartz dolerite (qd) (high grade gold) (Beeson, 2011).

The most obvious and widest shear zone is located within the Au-mineralized zone, forming a backbone structure within and immediately around which Au grades are highest (Fig. 2.3). The shear zone is a composite structure comprising penetratively foliated quartz-pyrite-albite-graphite breccias domains which enclose and grade into weakly to non-foliated domains of intense quartz-pyrite-albite brecciation; laminated quartz veins are also locally developed within this shear-breccia zone. Thus the Au-rich shear-breccia zone at Paboase comprises foliated breccias and brecciated foliated rock that appears to have formed during multiple, mutually overprinting foliation and brecciation episodes during the Au event (Beeson, 2011).

Paboase drill core contains a variety of brittle structures that in combination with the ductile to brittle-ductile structures define different structural domains in and adjacent to the Au zone. These structures include breccias networks, fracture sets, faults and veins. At least four structural domains expressed by the nature and intensity of deformation can be defined across Paboase, as follows (Beeson, 2011):

- Footwall breccia domain – this domain lies on the western (footwall) side of the mineralised domain (see below). It is characterised by widespread brecciation related

to quartz-dominant and albite-dominant veining (Fig. 2.4a) and intrusion of the intermediate-felsic suite (particularly quartz (feldspar) porphyry). The rocks in this domain are typically more strongly veined, altered and brecciated than the hangingwall sequence, rendering primary lithology recognition relatively more difficult in the footwall.

- Mineralised domain – this domain hosts the bulk of gold mineralisation at Paboase and is thus the focus of the gold resource. The mineralised domain includes the ductile- to brittle ductile shear-breccia as in Fig. 2.3 enclosed inside a domain of ankerite-albite-silica-(pyrite-graphite) breccias. These rocks are referred to locally as brown breccia, having a distinctive brown-yellow colour and being characterised by intense, commonly texturally-destructive alteration (Figure 2.4b-d). The ankerite-albite breccias form a skin around the backbone shear-breccia zone.
- Paboase Eastern Fault domain – this domain is the narrowest structural domain and lies immediately east of the mineralised domain in the hangingwall. This domain is characterised by a zone of broken, blocky ground enclosing a narrower zone of highly fractured ground and fault gouge that post-dates and locally shatters the brown breccias of the mineralised domain (Figs. 2.5a and 2.5b). Down-hole widths of this zone typically range from 2-10 m. In some cases the fault that defines this domain may be represented by two adjacent domains of broken ground and fault gouge (i.e. the fault locally bifurcates).
- Hangingwall domain – this domain lies immediately east of the Paboase Eastern Fault domain and is characterised by relatively mildly deformed rocks containing the following features (from oldest to youngest):
    - local intrusive breccias between tonalite and mafic rocks (Figs. 2.5d, 2.9c, 2.7a)

- narrow ductile to brittle-ductile chloritic shears (typically <1m down-hole width),
- fracture networks containing either hematite-albite, chlorite, silica or graphic K-feldspar quartz veins (Figures 2.9d, 2.8a, 2.8b) , and
- local zones of broken ground (generally <5-10m down-hole width) representing fault structures probably oriented sub-parallel to the Paboase Eastern Fault domain that appear to fan through particular rock units in the hangingwall.

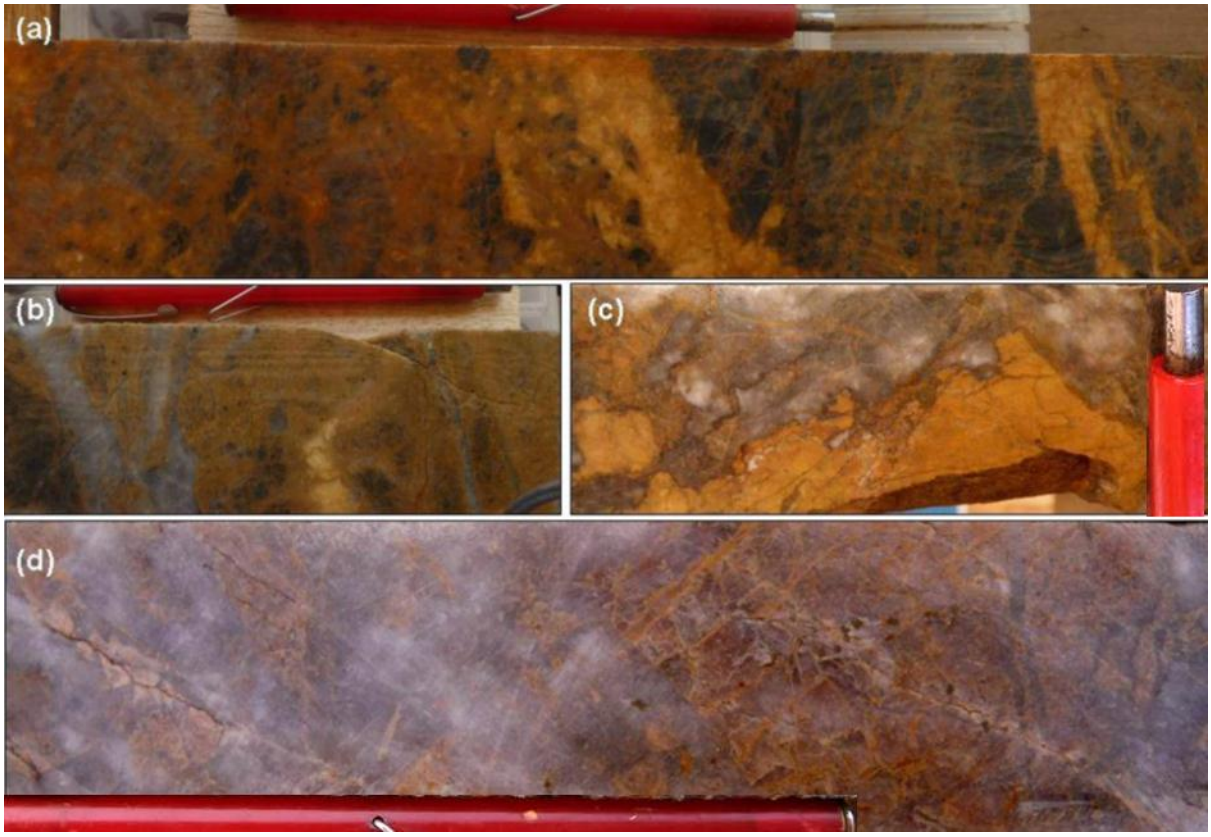

Fig. 2.4 (a) Typical breccias and vein-network present in the western (footwall) rock sequence at Paboase. Rocks in the footwall are generally more heavily altered than rocks in the hangingwall. (b) Ankerite-albite (brown) breccias from the mineralized domain. (c) Ankerite-albite breccias with grey quartz infill. (d) Ankerite-albite-silica-pyrite breccias from the mineralized domain cit by milky quartz breccias (Beeson, 2011).

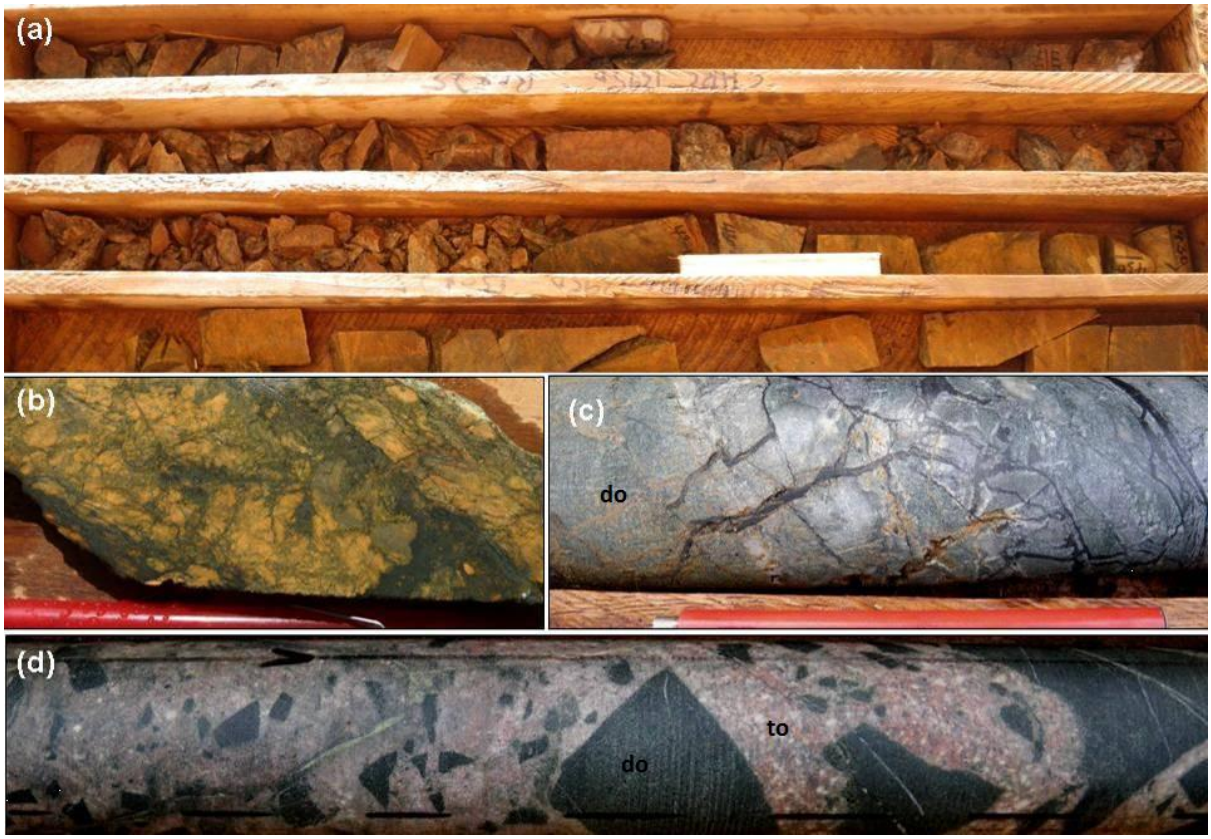

Fig. 2.5 (a) Fault zone bounding the mineralized domain on the eastern (hangingwall) side. (b) Paboase eastern fault cutting brown breccias of the mineralized domain. (c) Brecciated dolerite (do) with silica fracture-fill. (d) Tonalitic (to) intrusive breccias formed in dolerite (do) (Beeson, 2011).

Rock types encountered at Paboase can broadly be grouped into four according to Beeson (2011), namely mafic volcanic rocks, mafic intrusive rocks, intermediate-felsic intrusive rocks and late ultramafic (mafic) intrusive rocks.

2.3.1.1 Mafic Volcanic Rocks

Basaltic volcanic rocks are preserved as remnants of xenoliths within intrusive rocks. The basalt is generally equigranular and fine-grained and generally lacks well-preserved primary textures. In terms of volume the basaltic rocks are very minor, contrary to previous interpretations that basaltic rocks dominate the mafic sequences at Chirano. Alteration of the basalts comprises of pervasive chlorite-carbonate alteration forming a cryptically mottled

texture, as well as an irregular and relatively widely-spaced network of chloritic fractures. In general, basalt is preserved to the east of the Paboase mineralized zone (Beeson, 2011).

Fig. 2.6 Basalt showing chlorite-carbonate alteration and chloritic fractures (Beeson, 2011).

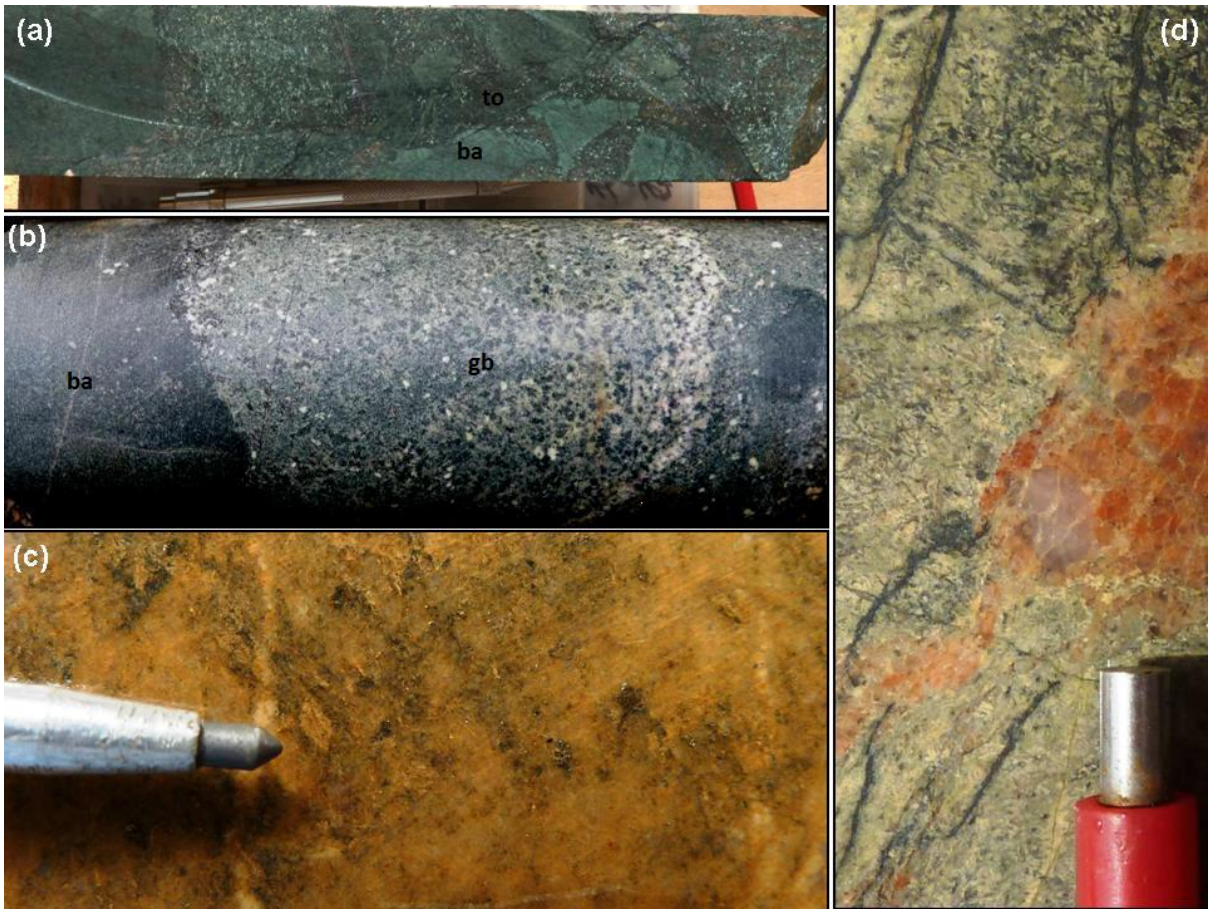

Fig. 2.7 (a) Tonalite (to) intrusive breccias hosting xenoliths of basalt (ba). White high-relief minerals in the tonalite are leucoxene after T-rich biotite. (b) Gabbroic (gb) rock intruding basalt (ba). (c) Quartz dolerite from the mineralized zone showing leucoxene after titano-magnetite and ankerite-albite-pyrite alteration. (d) Altered quartz dolerite showing bladed medium-grained texture and abundant skeletal to vaguely sub-equant yellowish-cream coloured leucoxene after titano-magnetite (Beeson, 2011).

2.3.1.2 Mafic Intrusive Rocks

The mafic rocks at Paboase are dominated by a mafic intrusive complex showing evidence of fractionation. The mafic intrusive rocks vary from gabbro, dolerite, to quartz dolerite (locally very quartz-rich). They locally host xenoliths of the basaltic sequence but in most instances appear to have obliterated the volcanic sequence (Beeson, 2011).

2.3.1.3 Intermediate-Felsic Intrusive Rocks

A diverse and widespread range of felsic to intermediate-felsic intrusive rocks is evident at Paboase intruding the basalt and the dolerite-gabbro intrusive rocks. These rocks are dominated by biotite-rich tonalite and various porphyritic rocks ranging from quartz-monzonite and quartz-alkaline feldspar granite to quartz syenite with decreasing age (Beeson, 2011). These rocks are described briefly below:

- Tonalite (granodiorite) intrusions comprise mostly biotite tonalite, but may tend towards granodiorite. The tonalitic intrusive rocks are volumetrically the most significant and the earliest of the felsic-intermediate intrusive suite. Later intrusive rocks consistently cross-cut and alter the tonalite. A large body of tonalite is evident in the structural hanging wall (east wall) of the deposit. This tonalite body appears to dip away from the mineralized zone at a moderate angle grid-east, becoming truncated against structures associated with mineralization to the west. Many tonalite intrusions show sharp contacts with dolerite and entrain basaltic xenoliths. Some tonalitic angular intrusive breccias are evident locally intruding the dolerite-gabbro. All of the tonalites at Paboase show signs of moderate to intense alteration (Beeson, 2011).

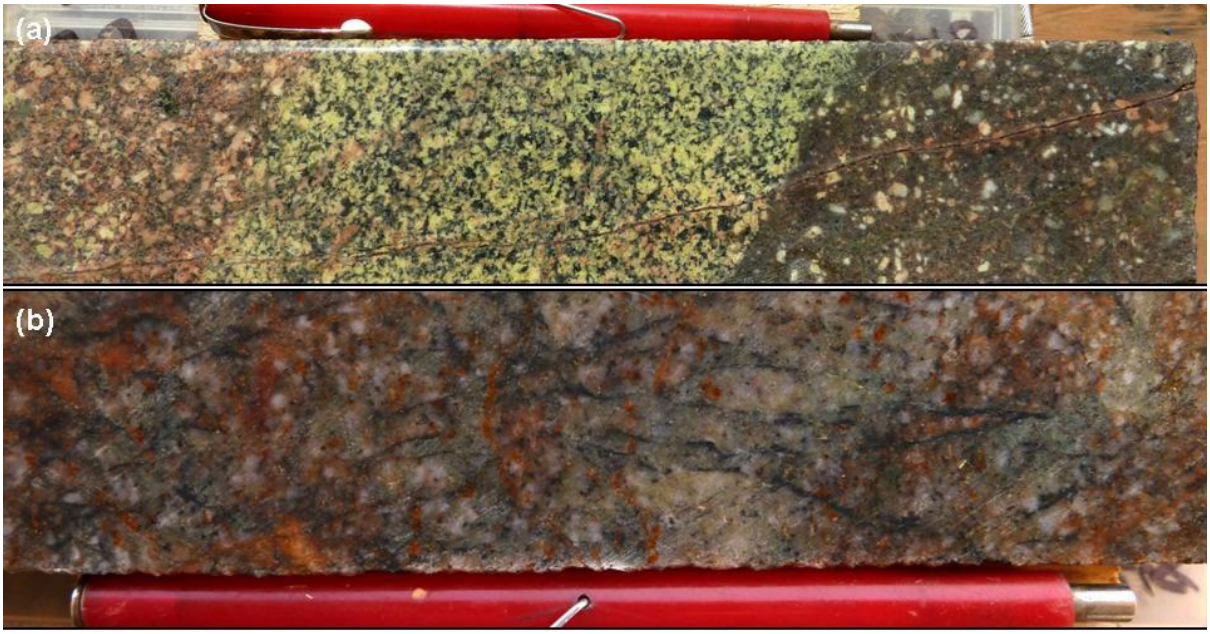

Fig. 2.8 (a) Biotite tonalite showing albite-silica-sericite-epidote alteration overprinted by albite-hematite alteration. The tonalite is intruded by a quartz monzonite (?) porphyry showing K-feldspar and quartz phenocrysts. (b) Biotite tonalite showing earlier albite-silica-sericite alteration overprinted by albite-hematite alteration (Beeson, 2011).

- Rhyolitic dykes – these rocks are located within and in close proximity to the Paboase mineralized zone. The rhyolitic dykes are characterized by a crypto-crystalline quartz-feldspar aggregate with rare sub-mm scale ghosted phenocrysts. Where present in the mineralized zone they typically occur as fragments or lenses.
- Quartz (feldspar) porphyry intrusions – these intrusions are typified by a quartz-rich composition and show both a quartz-crowded porphyritic texture and a commonly brecciated fine-grained siliceous matrix. These are relatively common in the mineralized zone at Paboase and in the structural wall (west side of the mineralized zone). Their typically brecciated nature suggests that they may have been relatively volatile-rich, possibly assisting brecciation during emplacement. In terms of timing the quartz (feldspar) porphyries are relatively late, being present as both breccia fragments and boudinaged lenses in the ore zone and much less commonly as dykes that cross-cut the ore zone (Beeson, 2011).

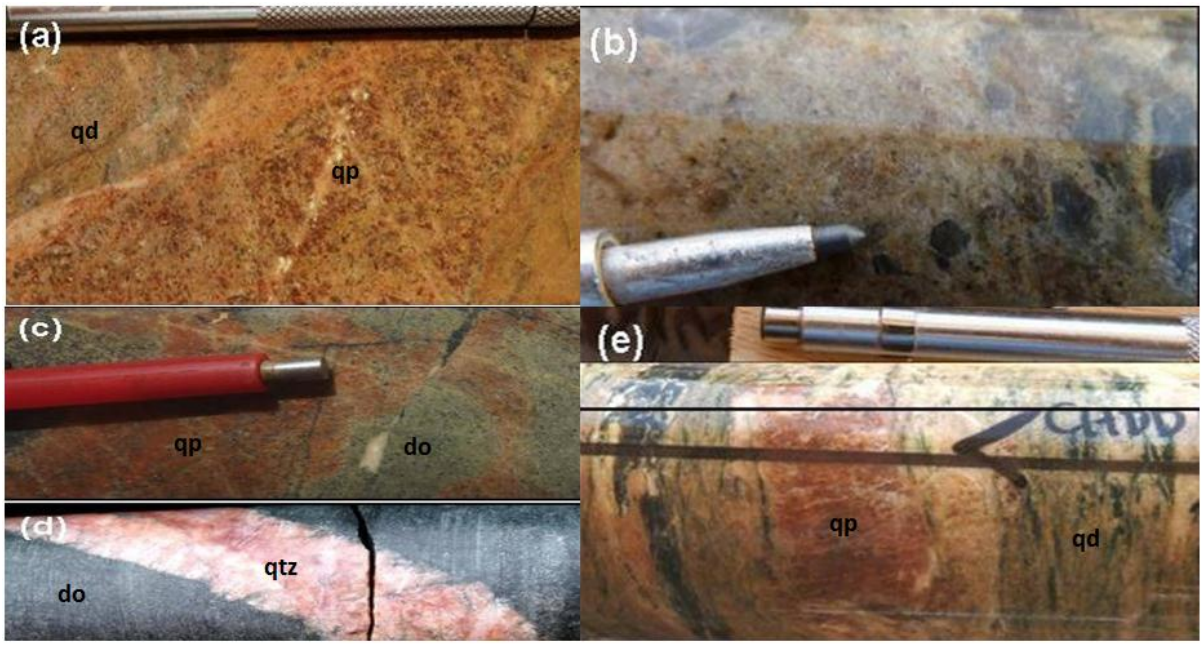

Fig. 2.9 (a) Quartz-feldspar porphyry (qp) intruding ankerite-albite altered quartz dolerite (qd) (brown breccia). (b) Quartz-feldspar porphyry showing hexagonal shape of quartz phenocrysts (orthogonal to crystal c-axis). (c) Quartz-feldspar porphyry (qp) intruding brecciated dolerite (do). (d) K-feldspar quartz (qtz) veins cutting dolerite (do). (e) Quartz-feldspar porphyry (qp) (pale pink lenses) intruding sheared and ankerite-albite-chlorite-(fuchsite) altered quartz dolerite (qd) (Beeson, 2011).

2.3.1.4 Late Ultramafic (Mafic) Intrusive Rocks

These are unusual potassic ultramafic intrusive rock and mafic intrusive rocks. There are at least three varieties of this rock evident at Paboase, and all members of this suite show very clear intrusive contacts, with well-developed chilled margins, where they intrude either the dolerite-gabbro suite or the intermediate-felsic intrusive suite. The three types of ultramafic intrusive comprise the following rock type; K-feldspar phyrric and phlogopite bladed lamprophyre, biotite lamprophyre with rare phlogopite phenocrysts and fine grained mafic/ultramafic intrusive (Beeson, 2011).

2.4 Multi-element Geochemistry

Major advances in analytical technology have occurred over the last four decades. Most notably, has been the introduction of inductively coupled plasma emission mass spectrometer (ICP-MS). When this ICP-MS technology is combined with inductively coupled plasma emission spectroscopy (ICP-OES) it offers a new formidable analytical technology. These advances have brought major and trace element geochemistry into the realm of being a cost effective, rapid and highly accurate means of solving complex geological situations (Actlabs, 2013). Lithogeochemical data could be used to establish some rock types (e.g. igneous rocks), subgroups of samples for further examination for alteration effects, indications of alteration and gain an indication of the process of mineralization (Franklin, 1999).

2.4.1 Lithogeochemistry

The geochemical analysis of host rocks can provide a template for the differentiation of individual rock units based on the variations in primary igneous chemistry. It can also define which elements are anomalous and the magnitude of anomalism caused by hydrothermal alterations. The combined results may define spatial scale of zonation that relate back to chemical variables such as pH, fO2 and aH2O that control Au and other metal grade distributions within the hydrothermal system (Micko, 2010).

Igneous compositional differences and hydrothermal alteration are the major material transfer processes that affect rocks in hydrothermal systems. In intensely altered rocks such as those found in this study area, elements representative of primary host rock composition that are immobile or high field strength elements (HFSE), such as Ce, Cr, Hf, La, Nb, Sc, Ta, Th, Ti, Y and Zr, can be utilized to discriminate primary compositions (Ciftci et al., 2005; Gale et al., 2002). These elements are commonly associated with silicate and phosphate host minerals,

formed during alteration, that are not refractory during acid dissolution. Zirconium, however, is the exception, as Phanerozoic zircon is generally refractory and may not completely dissolve in 4-acid geochemical package. Therefore, Zr may be under-reporting to the assay values, and thus must be used with care (Micko, 2010).

2.4.2 Mapping Rock Types

Halley (2011), stated that one way to fingerprint different rock units geochemically is to use scatter plots of immobile trace elements and that the most reliable immobile trace elements are the transition metals, REE's and actinide elements with ionic charges of 3+ or 4+. In Halley's work he said the immobile elements can be thought of as comprising 3 suites;

- a mafic suite (correlating with Fe); Ti, Sc, V
- a felsic suite (correlating with Si); Zr, Hf, Th, La, Ce, P, Nb, Ta
- an ultramafic suite (correlating with Mg) Cr, Ni

To geochemically classify the rock types in a lithogeochemical data set, the preferred method is to generate scatter plots that allow the recognition of discrete populations within the data (Halley, 2011). The best way to do this is to plot elements that have high concentrations in one type of rock against elements that have high concentrations in another rock type. By plotting elements of opposing character, it causes the data points to spread across the whole area of the plot. For example, consider Ti and Zr, basalts are high in Ti but low in Zr, so they will tend to plot towards the top left. Rhyolites are high in Zr but low in Ti, so they will tend to plot towards the bottom right. By plotting all of the mafic elements sequentially against all of the felsic elements, all of the separate populations in the data can be visualized (Halley, 2011). Scandium is generally immobile during metasomatism; therefore, Sc-scatterplots effectively discriminate not only the effects of alteration, but can also distinguish between

samples of felsic, intermediate, mafic, and even ultra-mafic composition (Halley et al., 2006; Prendergast, 2007).

2.5 ASD Terraspec Spectrometer

The instrument controller is a computer which manages the ASD spectroradiometer, stores data and processes the results (Fig. 2.10). The device uses the reflectance and absorption characteristics of minerals, rocks and vegetation between Visible and Infrared energy regions.

The terraspec can be used to measure the composition and abundance of a variety of alteration minerals. It operates in the short wavelength infrared region of the spectrum between 350 and 2500 nanometres. In this range, a number of chemical bonds in the minerals absorb energy corresponding to particular wavelengths of light, giving rise to reflectance profiles with sharp dips at those particular wavelengths. In the Short Wave Infrared range, the absorption features are due to water, hydroxyl bonds, carbonates and sulfates (Spectral International Inc., 2005).

Reflectance spectroscopy was discovered by the remote sensing community. Reflectance spectroscopy can be defined as the technique that uses the energy in the Visible (0.4-0.7), Near Infrared (0.7-1.3) and Short Wave Infrared (1.3-2.5µm) wavelength regions of the electromagnetic spectrum to analyse minerals. The science and techniques of reflectance spectroscopy are based on the spectral properties of materials. Certain atoms and molecules absorb energy as a function of their atomic structures. The manifestation of this takes the form of a reflectance spectrum, with absorption features, wavelength positions and distinctive profiles which can be used to identify minerals and organic phases (Spectral International Inc., 2005).

Fig. 2.10 ASD Terraspec and computer accessory.

Spectral reflectance characteristics of minerals are the result of different physical and chemical properties. Transitions between energy levels and compositional differences are manifested by absorption features at specific wavelengths. Several different electronic processes operate in the Visible to Short Wave Infrared region (Spectral International Inc., 2005). Each mineral detected within the Short Wave Infrared region has a fairly unique set of spectral characteristics combined into the reflectance spectrum. The features have characteristic frequencies or wavelength positions and band widths. Both the spectral features and the hull or background component are influenced by multiple variables.

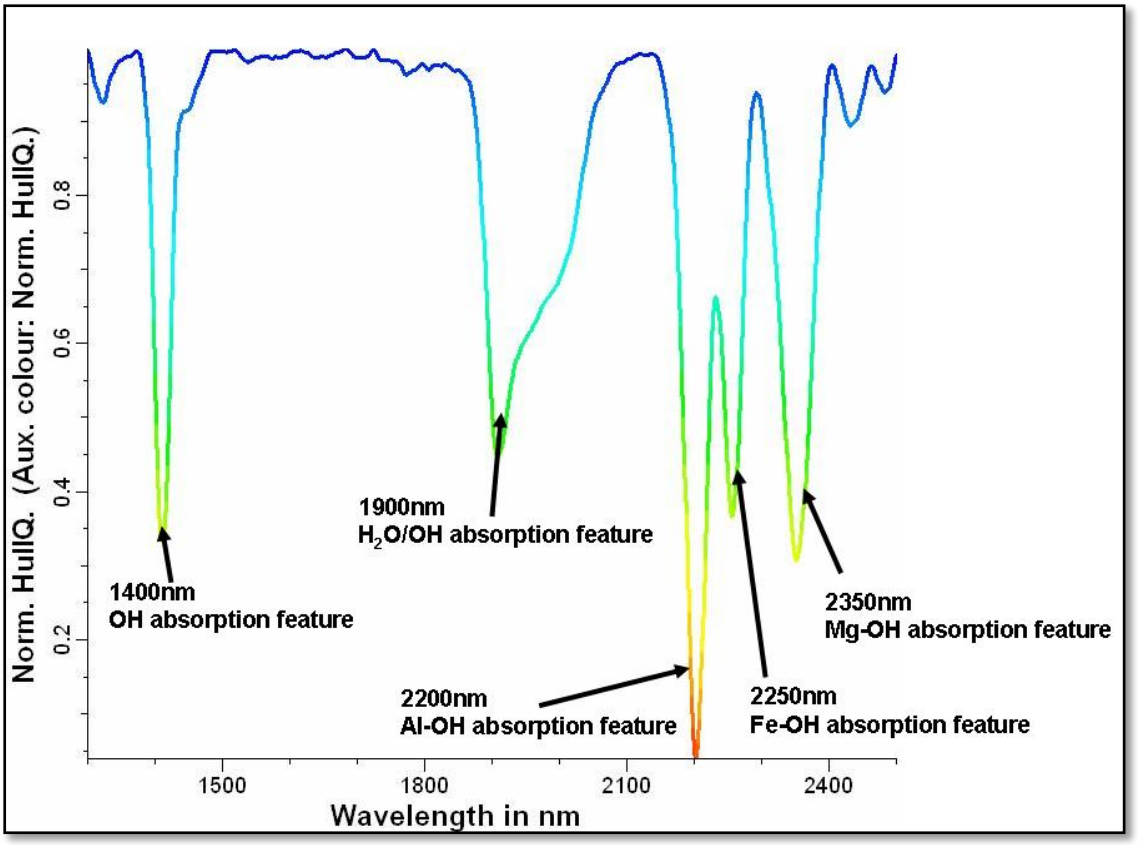

Fig. 2.11 Common spectral features.

Hydrothermal systems commonly have abundant chlorite and sericite. The absorption features of these minerals can be measured by the Terraspec and the various combinations of wavelengths and depths of these features correspond to different solid solution chemistry and proportions of those minerals. The way in which the sericite and chlorite respond to Short Wave Infrared is a reflection of the hydrothermal fluid chemistry from which those minerals were formed. When this is plotted in a spatial context, it often maps zonation patterns around hydrothermal alteration systems (Spectral International Inc., 2005).

2.5.1 Spectral Features of some Alteration Minerals

2.5.1.1 Sericite (Muscovite)

Sericite has an Al-OH absorption feature at about 2200 nm, a broad asymmetric H_2O feature at 1900 nm and an OH feature at 1400 nm (Fig. 2.12). The absorption features for the sericite

group minerals vary slightly from each other but they all have their major feature at around 2200 nm. The spectra of phengite are very similar to those of muscovite, with medium to major absorption features developed near 1410 nm, 1910 nm, 2200 nm, 2350 and 2445 nm. Phengite commonly has a weak shoulder on its long wavelength slope near 2240 nm (absent in muscovite). The absorption minimum of the 2200 nm feature has a variable wavelength. In acidic alteration environments where all the feldspar is replaced by sericite, the wavelength decreases to around 2195nm (Halley, 2011). In alkaline environments where new hydrothermal feldspar is created, the wavelength increases to more than 2215 nm (Halley, 2011). The sericite wavelength can be used as a pH indicator.

2.5.1.2 Chlorite

There are two major absorption features for chlorite: at 2260 nm and 2350 nm for Fe-chlorite; or at 2250 nm and 2330-2340 nm for Mg-chlorite (Fig. 2.13). Usually, the feature at 2330-2350 nm is asymmetric and 'fatter' than the symmetric one at 2250-2260 nm. Wavelengths of the two major features for chlorite of intermediate compositions vary between those of the above two extremes. The variation of the wavelength of the 2250 nm can be used as an indicator of the Fe to Mg ratio. Another significant feature, which also helps identify chlorite, occurs near 2000 nm. Other less significant features are those near 1390 nm and 1430 nm (Halley, 2011).

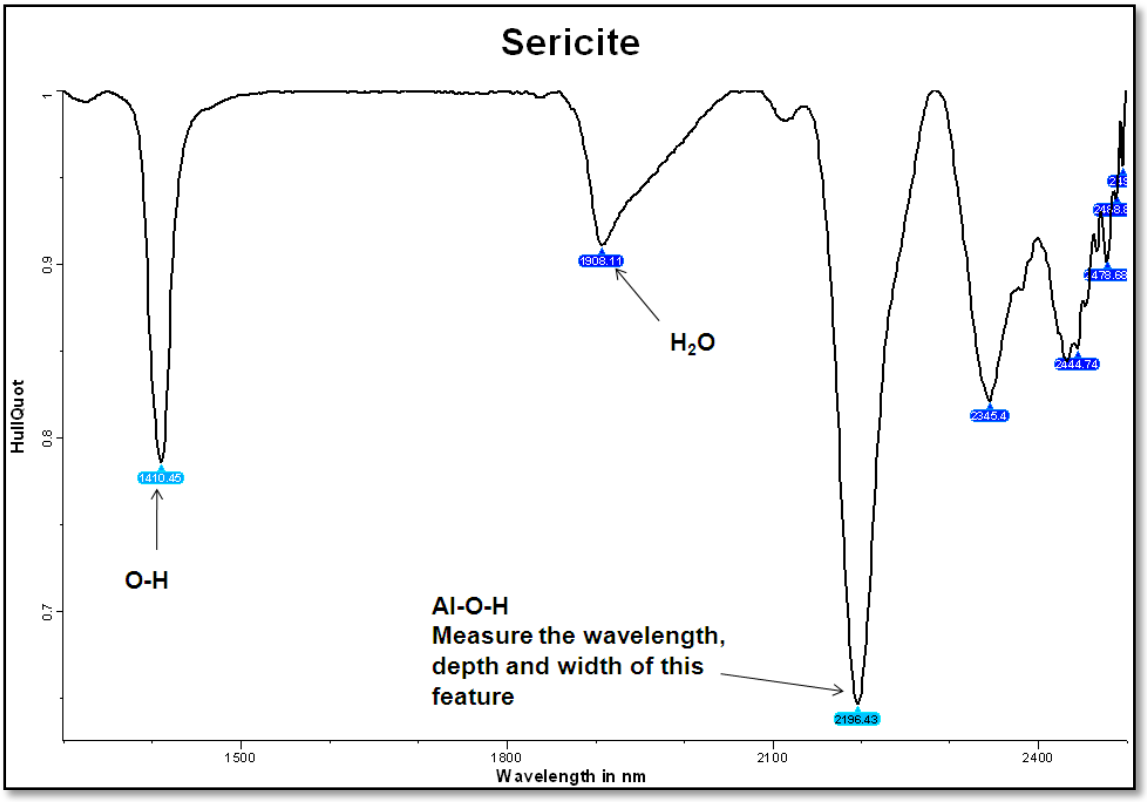

Fig. 2.12 Sericite absorption features.

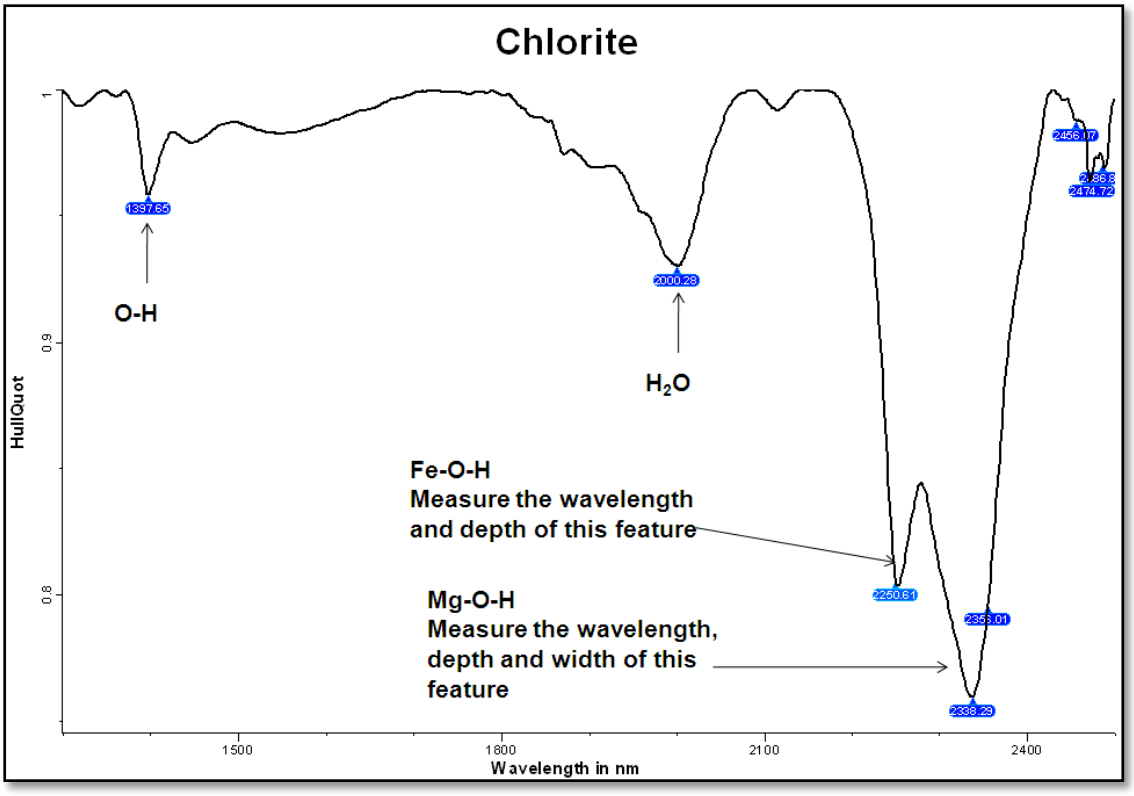

Fig. 2.13 Chlorite absorption features.

2.5.1.3 Carbonate

Carbonate minerals have an asymmetric absorption feature with a minimum value ranging from 2325 nm in dolomite, 2332 nm in ankerite and 2340 nm in calcite as shown in Figure 2.14 (Halley, 2011).

2.5.1.4 Epidote

Epidote usually gives clear, strong absorption features. The major feature is near 2340 nm with a sharp, but lesser, absorption near 2258 nm (Fig. 2.15). In these respects it is similar to chlorite, with which it can sometimes be confused. Epidote, however, has its third most diagnostic feature near 1550 nm and fourth feature near 1884 nm. In dry samples features near 1940 nm and 1946 nm may be also visible (Halley, 2011).

2.2.1.5 Mineral Mixtures

These are spectral that shows more than one major absorption features as in Figure 2.16 and 2.17. They could have sericite as mineral one and chlorite as mineral two or chlorite as mineral one and sericite as mineral two etc (Halley, 2011).

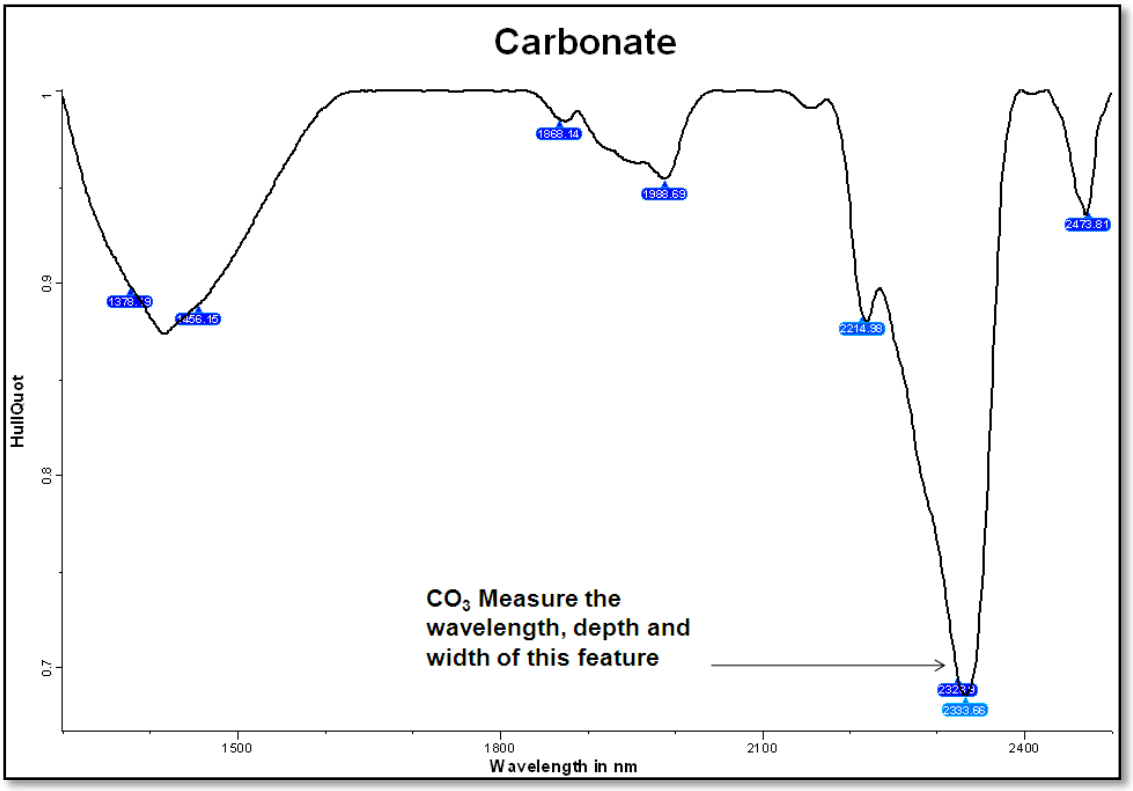

Fig. 2.14 Carbonate absorption features.

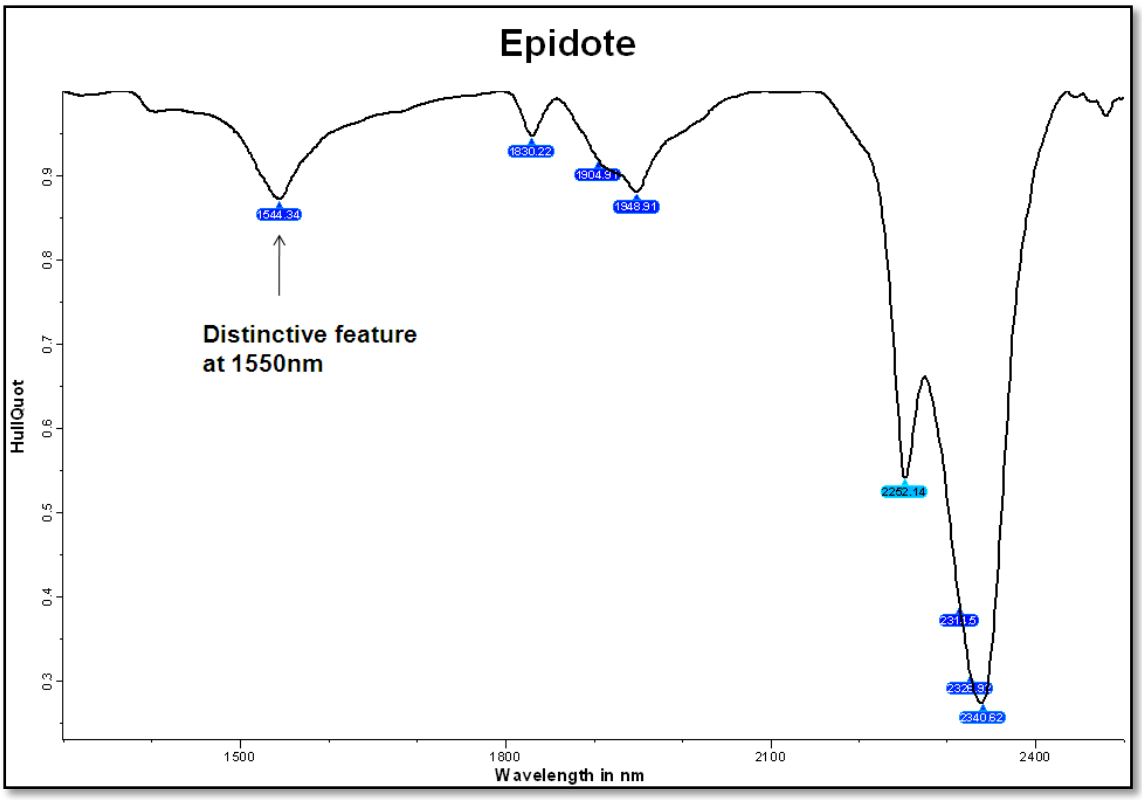

Fig. 2.15 Epidote absorption features.

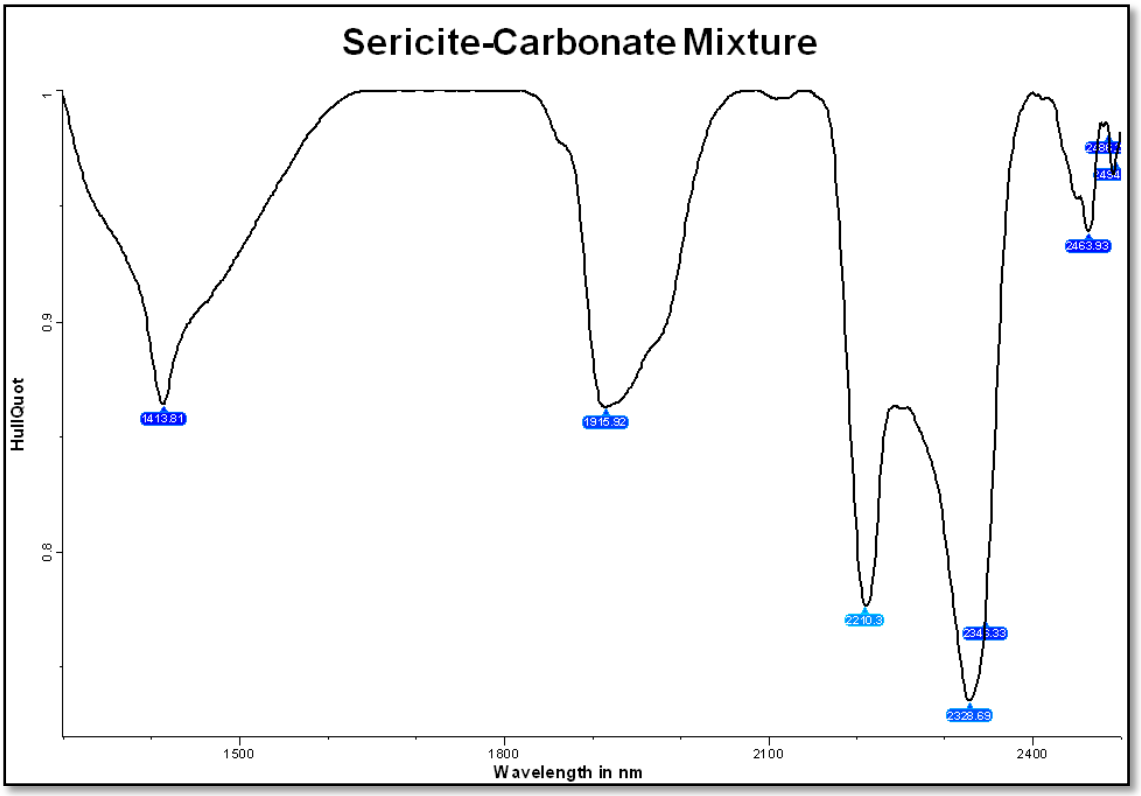

Fig. 2.16 Sericite-Carbonate mixture features.

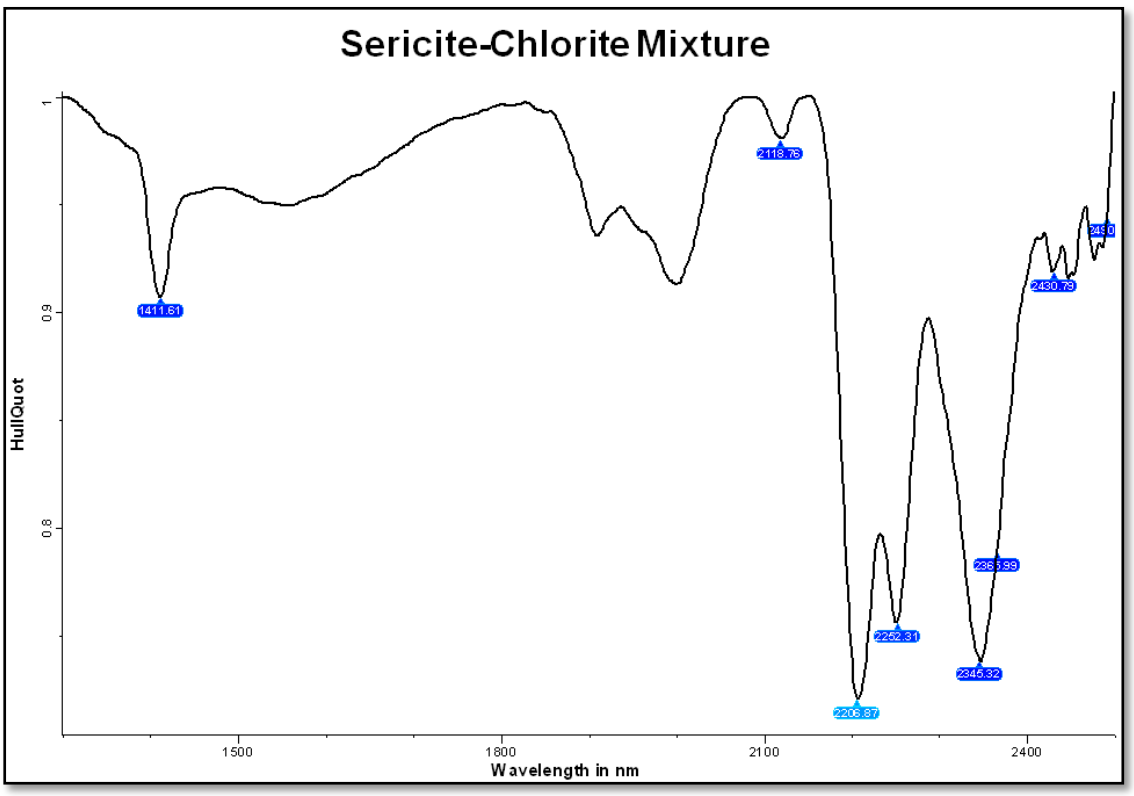

Fig. 2.17 Sericite-Chlorite mixture features.

CHAPTER THREE

METHODOLOGY

The project used two main data from the Paboase deposit; multi-element assays of selected drill holes on each section of 50 m drill spacing and Analytical Spectral Device (ASD) TerraSpec Spectrometer data collected from all the drilled holes.

3.1 Chirano Multi-element Survey

A multielement geochemical survey has been undertaken for selected holes on almost all drilled sections. Diamond drill core samples from the deposit drilled in 50 meters grid spacing were used. Samples have been taken on close spacing through the ore zones, usually on one, two or three meter spacing and on wider spacing of five meters into the country rock. Rather than quartering the drill core, sample pulps from the gold assays have been retrieved and resubmitted for analysis. The sample pulps were prepared by ALS Kumasi laboratory which earlier did the gold analysis. The sample preparation involves weighing, drying, crushing to 70% less than 2mm, riffle split off 250g, pulverize split to better than 85% passing 75 microns.

In all a total of 3,243 samples were analysed by ALS Chemex Vancouver using their Inductively Coupled Plasma – Mass Spectrometry (ICP-MS) and Inductively Coupled Plasma – Atomic Emission Spectroscopy (ICP-AES) methods. A prepared sample (0.25 g) is digested with perchloric, nitric and hydrofluoric acids (HF-HNO3-HClO4). The residue is leached with dilute hydrochloric acid and diluted to volume. During the digest, the solution is boiled until dry and then leached with HCl. This digest achieves very close to a near total digest in the majority of cases. It is then analysed by inductively coupled plasma-atomic emission spectrometry and inductively coupled plasma-mass spectrometry. Results are

corrected for spectral inter-element interferences. It must be noted that four acid digestions are able to dissolve most minerals; however, although the term "near-total" is used, depending on the sample matrix, not all elements are quantitatively extracted. For instance zircon and tin oxides are not completely dissolved in some cases.

Samples were analysed by following standard analytical procedures conducted through rigorous quality control checks as part of the laboratory accreditation. The ALS laboratories are accredited to ISO/IEC 17025-2005 standards to provide complete assurance regarding quality performance (ALS minerals Schedule of Services and Fees brochure, 2012). The lab package used, elements analysed and their correspondence detection limits are summarized in Table 3.1.

Table 3.1 Suite of elements analysed and reported minimum to maximum detection ranges for the ALS Chemex 4-acid digestion analysis using analytical package ME-MS61 and instruments ICP-MS and ICP-AES.

Element	Units	Lower Limit	Upper Limit
Ag	ppm	0.01	100
Al	%	0.01	50
As	ppm	0.2	10 000
Ba	ppm	10	10 000
Be	ppm	0.05	1 000
Bi	ppm	0.01	10 000
Ca	%	0.01	50
Cd	ppm	0.02	1 000
Ce	ppm	0.01	500
Co	ppm	0.1	10 000
Cr	ppm	1	10 000
Cs	ppm	0.05	500
Cu	ppm	0.2	10 000
Fe	%	0.01	50
Ga	ppm	0.05	10 000

Table 3.1 (contd.)

Element	Units	Lower Limit	Upper Limit
Ge	ppm	0.05	500
Hf	ppm	0.1	500
In	ppm	0.005	500
K	%	0.01	10
La	ppm	0.5	10 000
Li	ppm	0.2	10 000
Mg	%	0.01	50
Mn	ppm	5	100 000
Mo	ppm	0.05	10 000
Na	%	0.01	10
Nb	ppm	0.1	500
Ni	ppm	0.2	10 000
P	ppm	10	10 000
Pb	ppm	0.5	10 000
Rb	ppm	0.1	10 000
Re	ppm	0.002	50
S	%	0.01	10
Sb	ppm	0.05	10 000
Sc	ppm	0.1	10 000
Se	ppm	1	1 000
Sn	ppm	0.2	500
Sr	ppm	0.2	10 000
Ta	ppm	0.05	100
Te	ppm	0.05	500
Th	ppm	0.2	10 000
Ti	%	0.005	10
Tl	ppm	0.02	10 000
U	ppm	0.1	10 000
V	ppm	1	10 000
W	ppm	0.1	10 000
Y	ppm	0.1	500
Zn	ppm	2	10 000
Zr	ppm	0.5	500

3.2 ASD Data Collection and Processing

The three most useful maps that we can generate from the Terraspec data are maps of alteration minerals, illite chemistry and chlorite chemistry.

Data collected was from about 80% of both Reverse Circulation (RC) and diamond drilled core (DD) drilled in the Paboase deposit. An average of one spectrum per meter was measured from 226 RC and 189 DD holes. A total of 57,107 spectra measurements were used for the project.

Fig. 3.1 Measuring spectral data using ASD Terraspec Spectrometer.

The raw data collected by the Terraspec was processed in 'The Spectral Geologist' (TSG) software. TSG matches the sample spectra to the correct mineral types. It has a routine built into it called "The Spectral Analyst" (TSA) which mathematically matches the sample spectra to reference library spectra. It will find the best mathematical match between the sample spectra and a reference spectrum or weighted combination of two spectra. TSA reports a mineral or combination of two minerals that most closely match against the sample spectrum. It also reports the relative weighting of each mineral that it has used for the match (TSA_Mineral 1, TSA_Weight 1 and TSA_Mineral 2, TSA_Weight 2). It also reports a mathematical result which describes how well it has matched the reference spectra to the sample spectra (TSA_Error). If the error result is above a pre-set threshold, it reports the mineral match result as Aspectral (no match).

However, TSG generates complex mineral names and subdivides mineral types in lots of sub-species. Also, when there are poor quality spectra, TSG will come up with some strange options as the best mineral matches. Rather than having very complex legends on the mineralogy maps, some of the mineral types have been grouped in ioGAS software in the following way:

- Sericite includes; Illitic Muscovite, Illitic Paragonite, Illitic Phengite, Muscovite, Paragonite and Phengite.
- Chlorite includes; Fe-Chlorite, Fe-Mg-Chlorite and Mg-Chlorite.
- Amphibole includes; Hornblende, Actinolite and Riebekite.
- Montmorillonite includes; Montmorillonite and Palygorskite.
- Carbonate includes; calcite, dolomite ankerite and siderite.

CHAPTER FOUR

RESULTS

This chapter deals with the results obtained using scatter plots of immobile trace elements to geochemically classify rock types in a lithogeochemical data set. One way to do this is to plot elements that have high concentrations in one type of rock against elements that have high concentrations in another type of rock (Halley, 2011). By plotting elements of opposing character, it causes the data points to spread across the whole area of the plot thereby allowing the recognition of discrete populations within the data (Micko, 2010; Halley, 2011). In addition, there are major element molar ternary and molar ratio plots to determine the alteration mineralogy and probability plots to show how pathfinder metal distributions correlates with alteration mineralogy.

4.1 Immobile Trace Element Plots

The plots in Figure 4.1a and 4.1b show Sc versus Zr, Th, Nb and Al. In the plot a simplified logging code was used to colour scatter plots of immobile trace element chemistry. The point density overlay is an aid to help visualize the clusters within the data. Two populations can clearly be seen; a mafic group circled in green and a felsic group circled in red. One advantage of using scandium in these plots is that it substitutes for Fe in silicate minerals (Fig. 4.2) but it is far less mobile than Fe (Halley, 2011). Fe may be quite mobile during alteration and weathering. Also, scandium is relatively immobile during metasomatism; therefore, Sc-scatter plots effectively discriminate not only the effects of alteration, but can also distinguish between samples of felsic, intermediate, mafic and even ultra-mafic composition (Halley and Walshe, 2006; Prendergast, 2007). Therefore, the abundance of Sc is a proxy for the relative abundance of pyroxene, amphibole, chlorite, biotite, i.e. Fe-Mg

minerals prior to the alteration event (Halley and Walshe, 2006; Neumayr et al., 2006; Walshe et al., 2006).

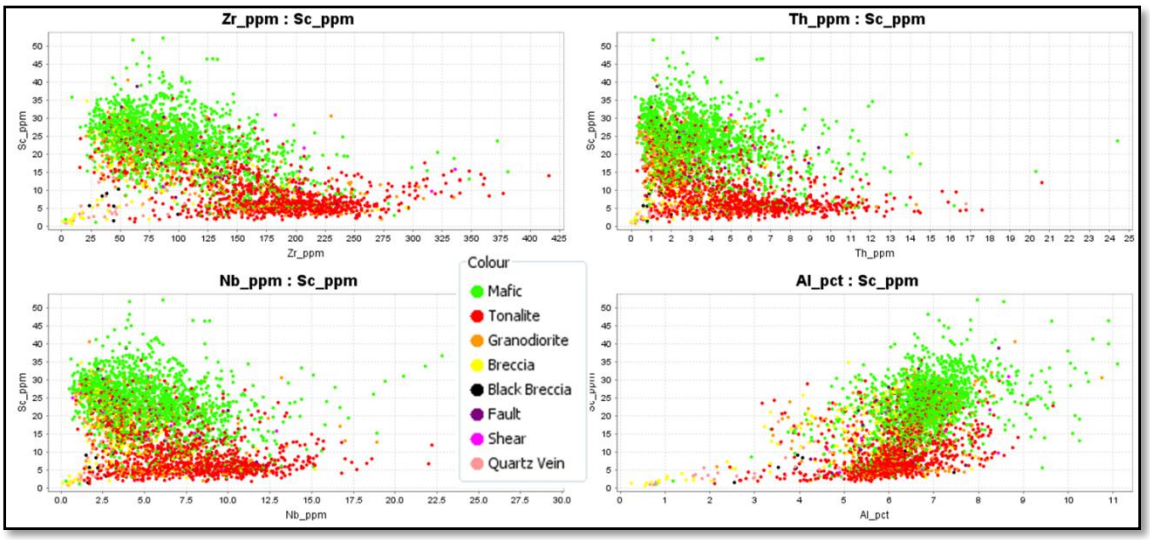

Fig. 4.1a Immobile trace element scatter plots of Sc versus Zr, Th, Nb and Al; colours based on logging codes.

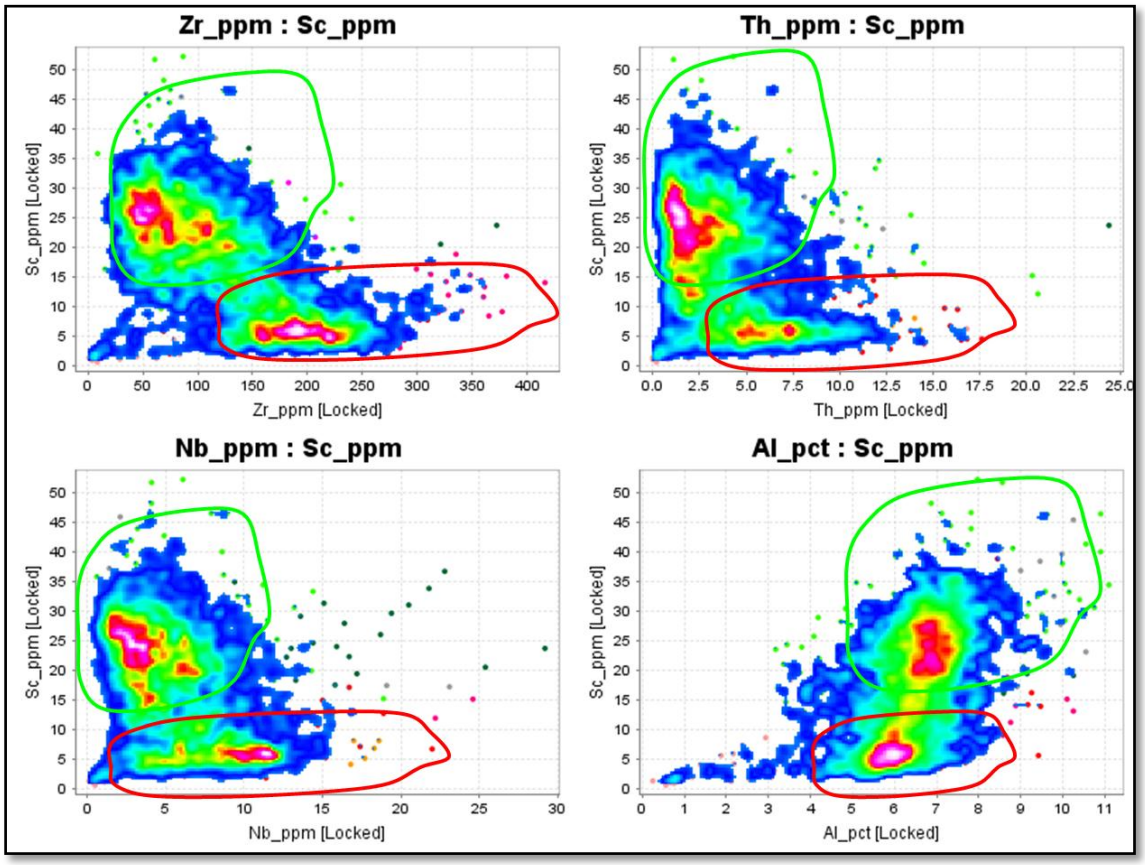

Fig. 4.1b Immobile trace element scatter plots of Sc versus Zr, Th, Nb and Al; coloured based on logging codes with point density overlay.

It can be seen from Figures 4.1a and 4.3a that there are some of the logging data that do not match the chemistry (reds and greens overlapping), mafic rocks that have been logged as felsic and some few felsic rocks that have also been logged as mafic. Sc values in mafic rock units are higher than the values in felsic to intermediate rock units. An empirically defined boundary lies at Sc = 20 ppm (Micko, 2010). Sc values ranging between <1 and 10ppm discriminate felsic intrusive suite from intermediate suite that dominantly ranges from 10 to 20 ppm (Figure 4.1a). As a rule of thumb, basalt will have 30 to 40 ppm Sc, andesite 20 to 30 ppm, dacite 10 to 20 ppm and rhyolite 0 to 10 ppm (Halley, 2011). The plots can therefore be refined to correct the wrongly logged rocks using the geochemistry data (Figure 4.3b).

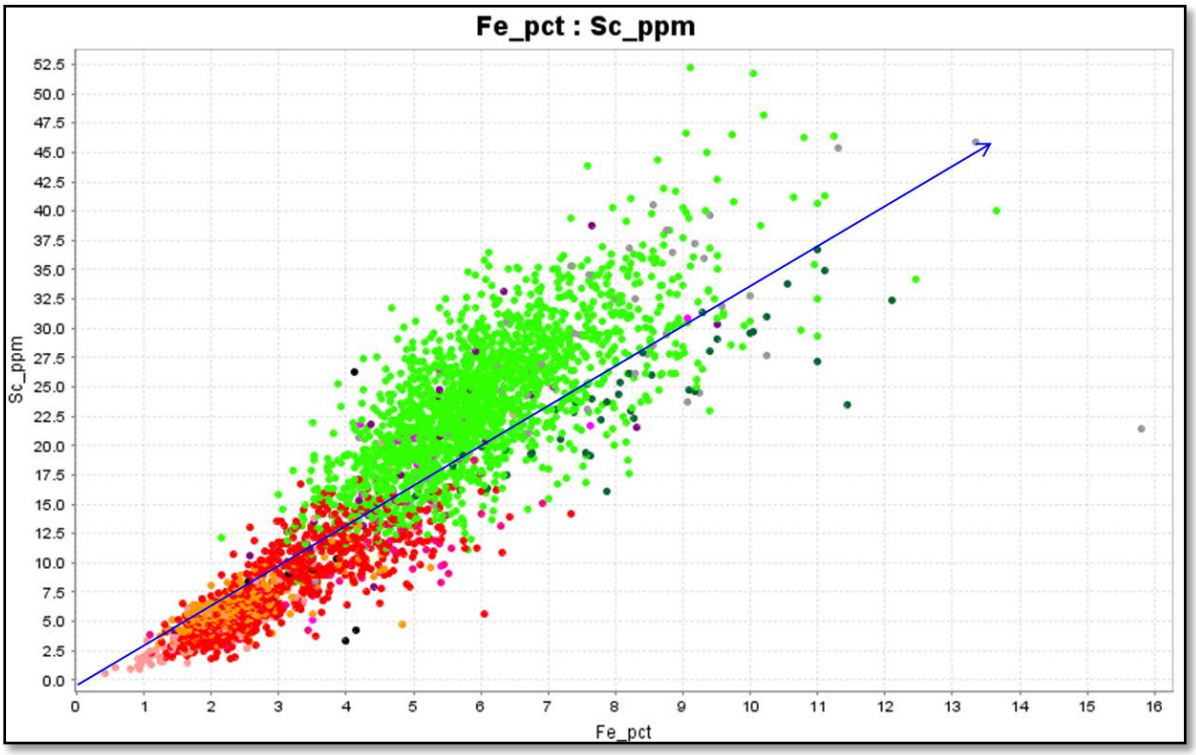

Fig. 4.2 Linear correlation between Sc and Fe.

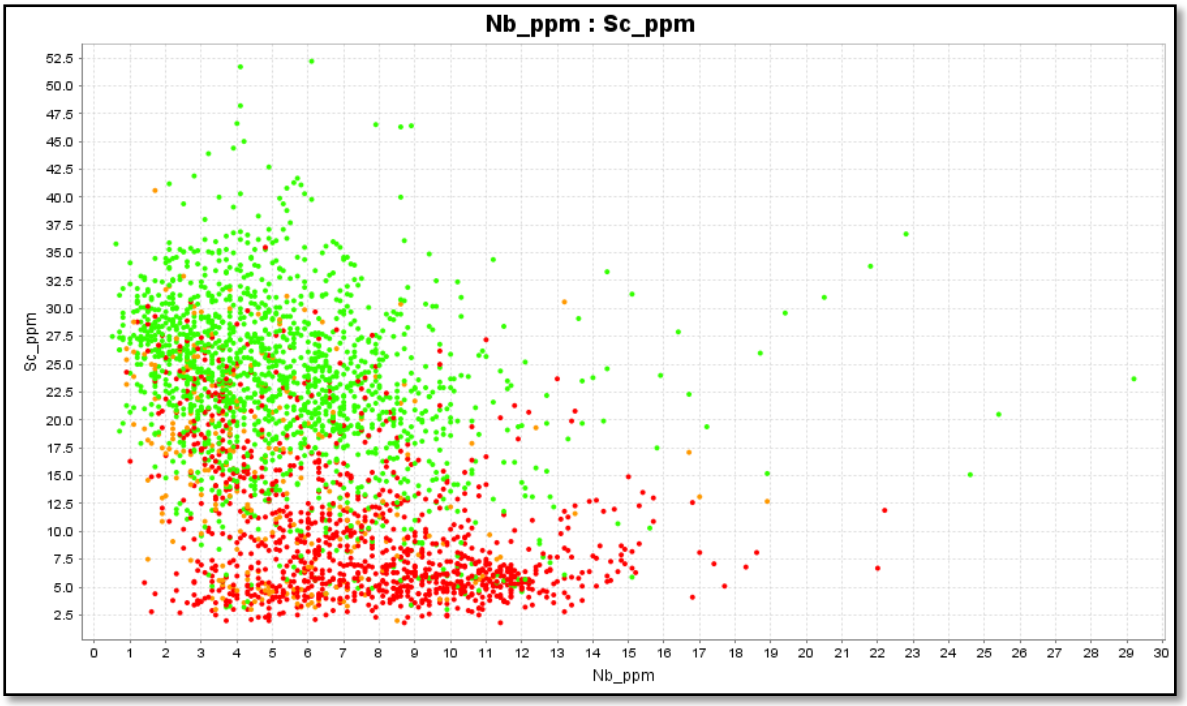

Fig. 4.3a Immobile trace element scatter plot of Sc versus Nb showing mafic and felsic rocks incorrectly logged.

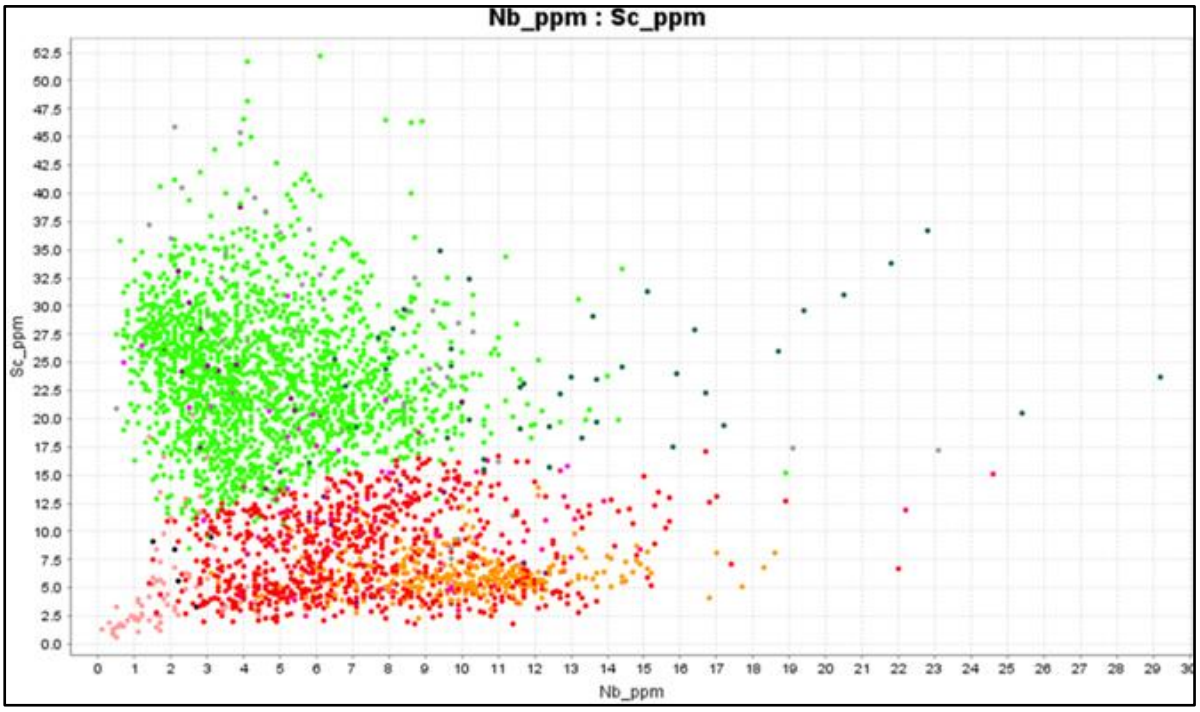

Fig. 4.3b Plots showing logging codes refined using point clusters in the immobile elements.

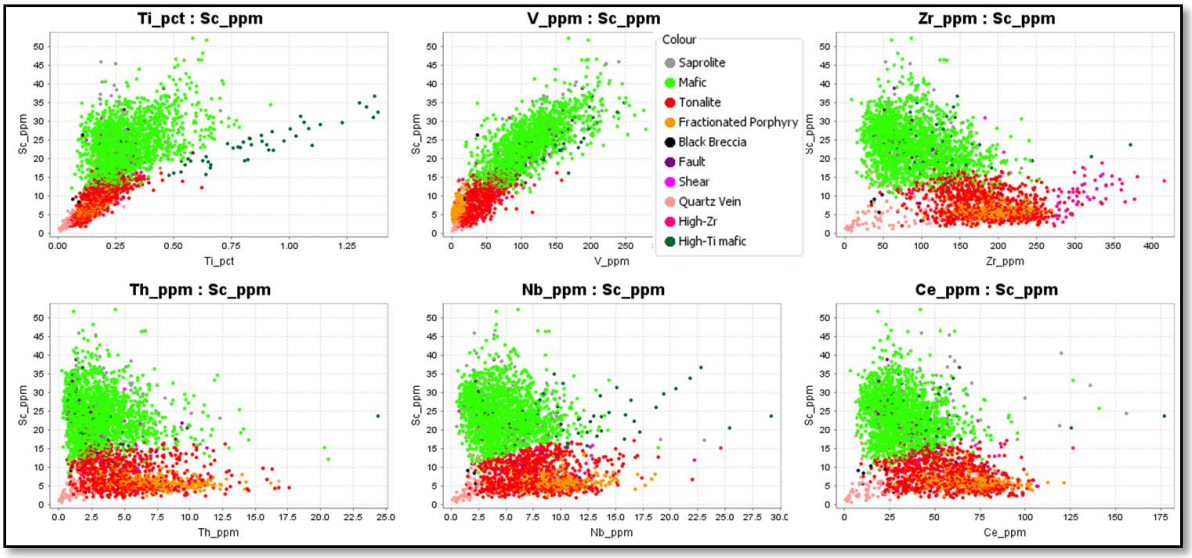

Fig. 4.3c Immobile elements plot of Sc versus Ti, V, Zr, Th, Nb and Ce after it has been refined.

4.1.1 Mafic Rock Units

Figure 4.4 shows the rocks logged as basalt (pale green) and rocks logged as dolerite, quartz dolerite or gabbro (dark green). Fine grained and coarse-grained mafic rocks are geochemically identical.

There is a small population of samples with very high Ti content. These are selected in Figure 4.3c as dark green. In Figure 4.5, the drill holes names are plotted against depth down hole, and the points are coloured by the chemical signatures of the mafic rocks defined in Figure 4.4. The exotic mafic group (high Ti) occur in short intervals in just some few holes. This is a small, late, cross-cutting dyke, perhaps with lamprophyre affinity.

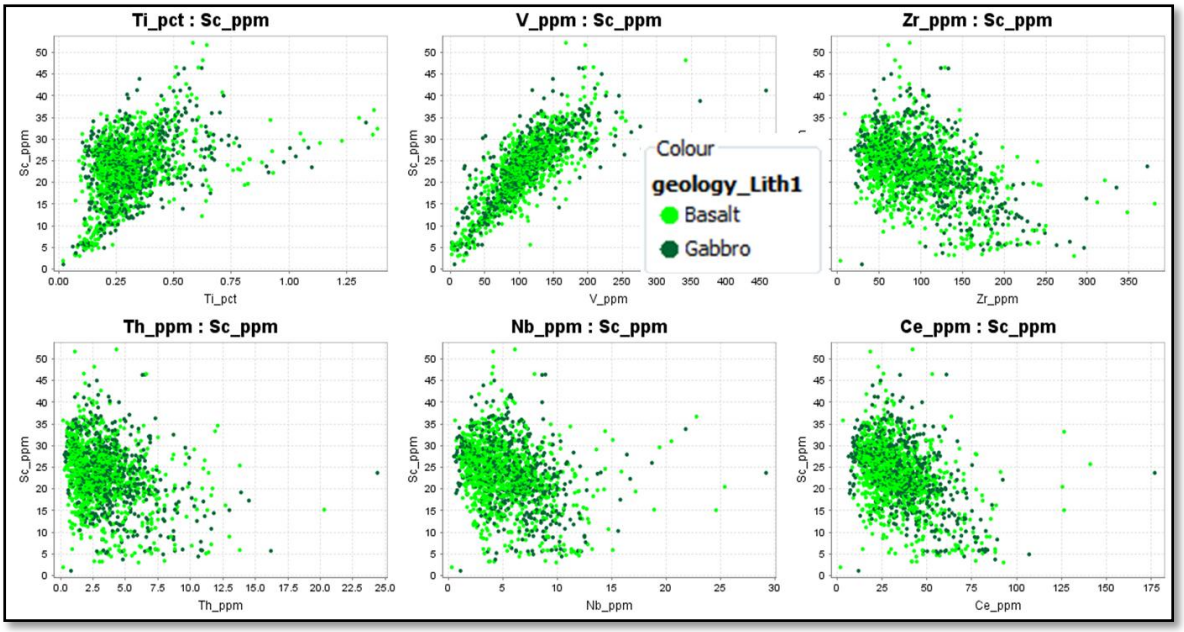

Fig. 4.4 Sc versus Ti, V, Zr, Th, Nb and Ce showing the compositon of fine grained and coarse-grained mafic rocks.

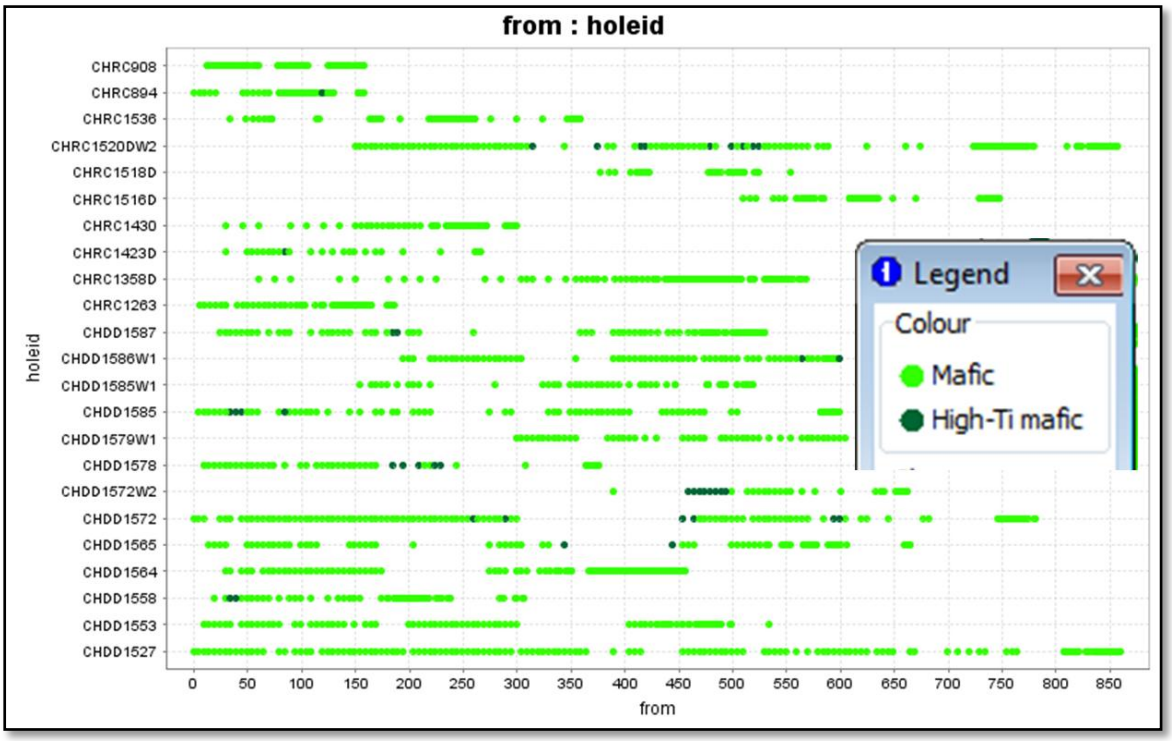

Fig. 4.5 Drillhole name versus depth of hole plot showing location of small volume mafic unit.

4.1.2 Felsic Rock Units

The plot in Figure 4.6 shows some of the different felsic units. The red group is the rock logged as tonalite or granodiorite. Scandium and vanadium usually have a very linear correlation trend as indicated by the arrow. There is one felsic unit that has low V relative to Sc (highlighted by the point density contours). This is a felsic magma that has had fractional crystallization of magnetite. These magma have probably fractionated magnetite in the parental magma chamber (thus become vanadium depleted) prior to the emplacement of this porphyry.

There is a small cluster of points in Figure 4.3c of zircon-rich that have been highlighted in the pink colour. This plot as a spatially coherent group of points and it is a second porphyry composition.

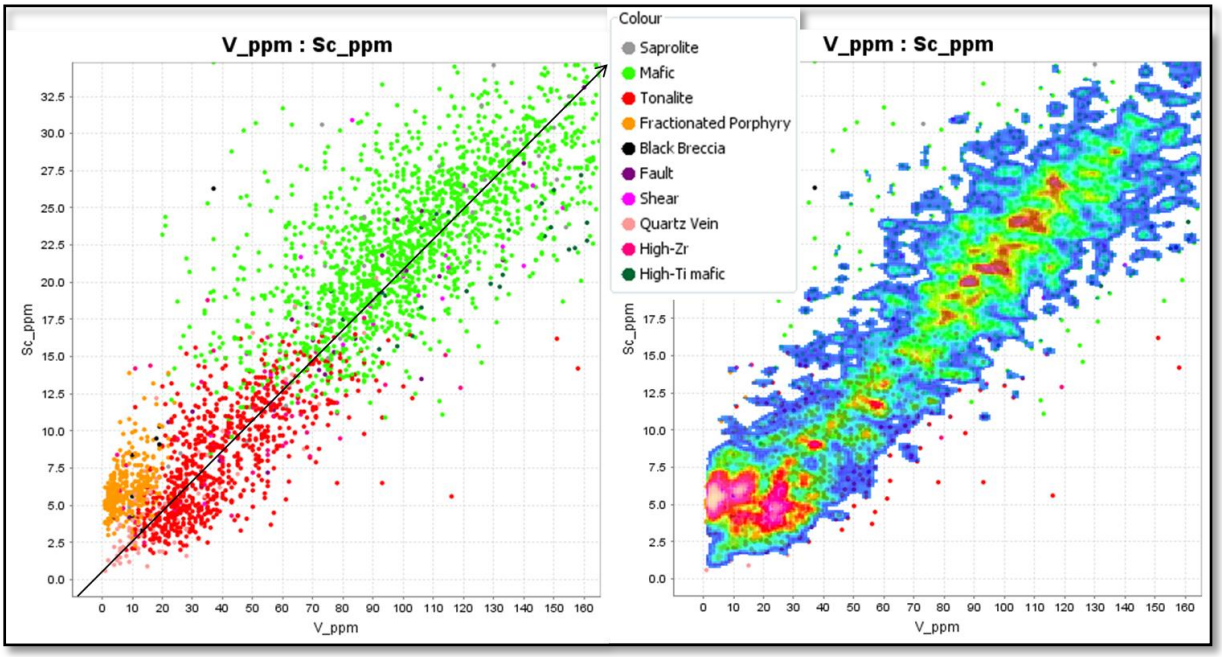

Fig. 4.6 A plot showing different felsic units.

4.2 Geochemistry Alteration Mineralogy

4.2.1 Feldspar-Sericite K/Al vs Na/Al Molar Ratio Plot

Major element molar ternary and molar ratio plots can examine not only igneous compositional changes, but also the superposed effects of hydrothermal alteration. Major elements prominent in the study area are K, Al and Na associated with igneous and/or hydrothermal mineral assemblages (Halley, 2011). By plotting the ratio of K/Al versus Na/Al, the alteration mineralogy can be inferred. These are ratios calculated on a molar proportion rather than a weight percent basis (Halley, 2011). This allows the data to be projected in terms of alteration mineral compositions. In this way, the relative amount of sericite, or albite can be quantified. Before the amount of sericite or albite that has been added or removed can be calculated, the initial starting composition of each rock type has to be determined, or estimated. Each rock type has a different initial ratio for these elements, so each group has to be plotted one by one.

The mafic rocks show two different alteration paths. Most of the rocks are altered towards the composition of albite and others towards the composition of muscovite (sericite). As basalts become more altered, they gain more potassium forming sericite (Halley, 2011). In most of the basalts, the sericite is then replaced by albite and they react to the lower right corner of the diagram (Fig. 4.7). According to Halley, a relatively alkaline fluid is required to make hydrothermal feldspar and acidic fluid to sericitise the rock.

The felsic rocks also showed a similar reaction path; most of the rocks are altered towards the composition of albite and others towards muscovite (sericite) (Figs. 4.8 and 4.9).

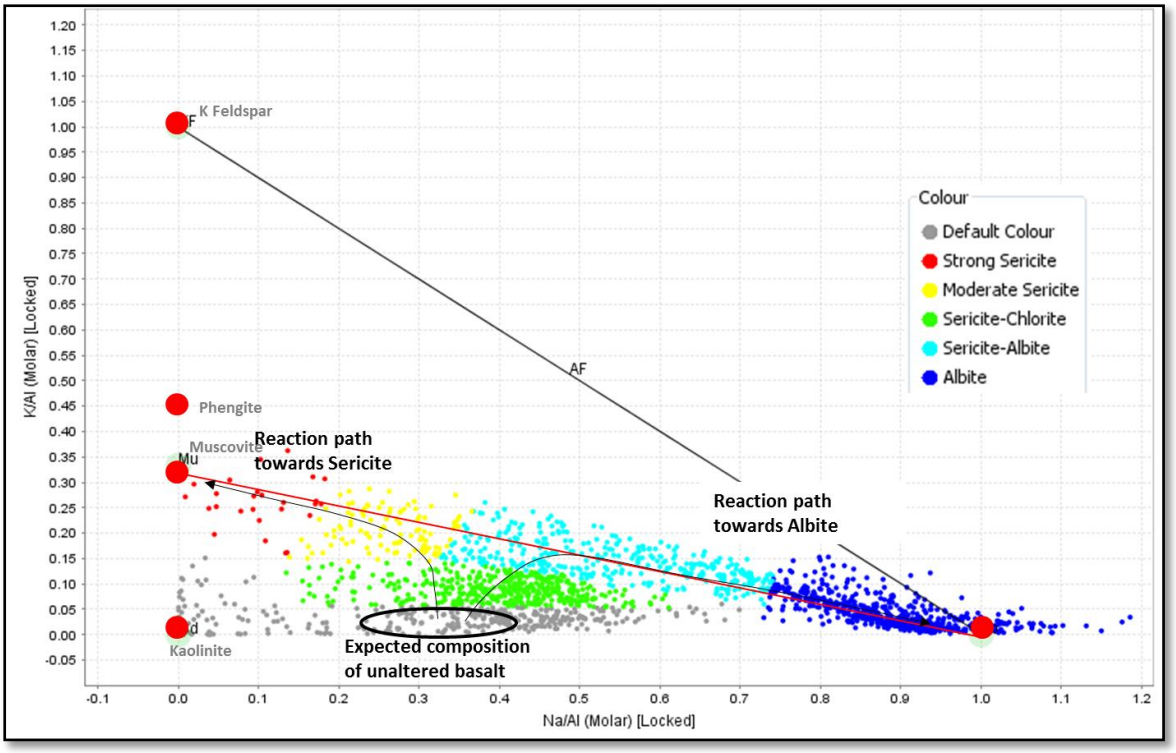

Fig. 4.7 Molar K-Al-Na ratio plot identifying the projected alteration signatures of the mafic rocks with the help of element ratio tie lines.

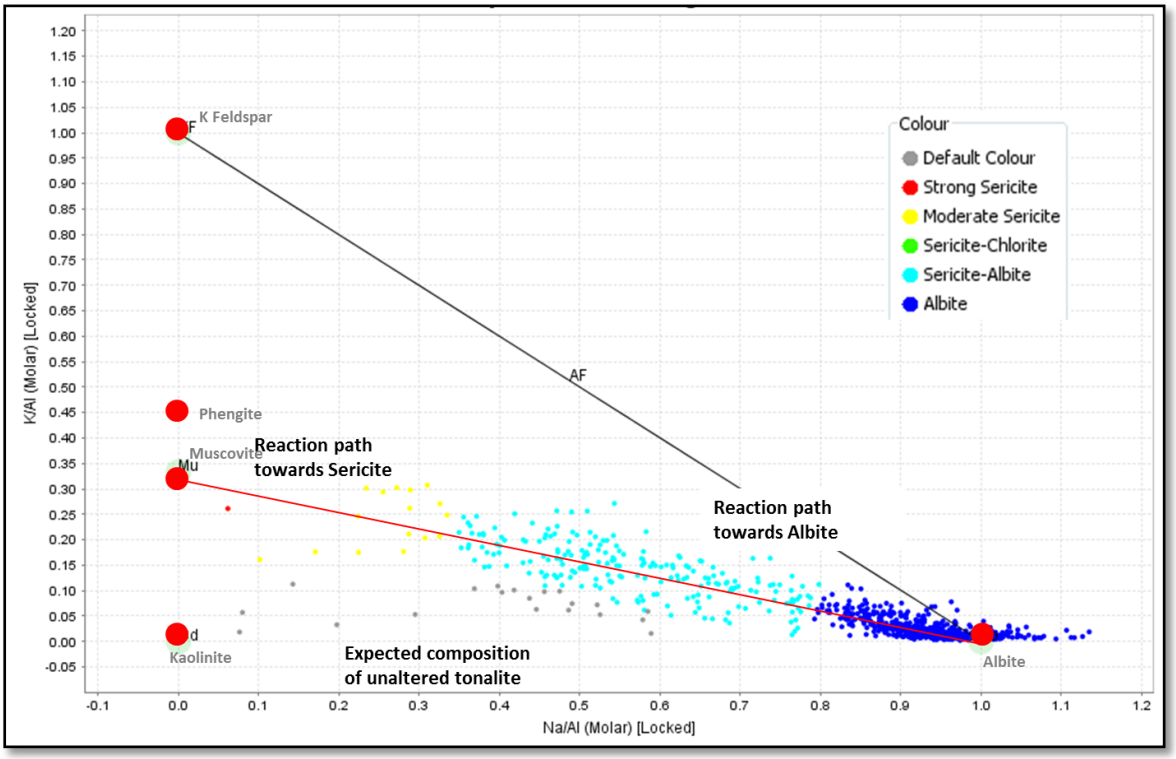

Fig. 4.8 Molar K-Al-Na ratio plot identifying the projected alteration signatures of the felsic rocks with the help of element ratio tie lines.

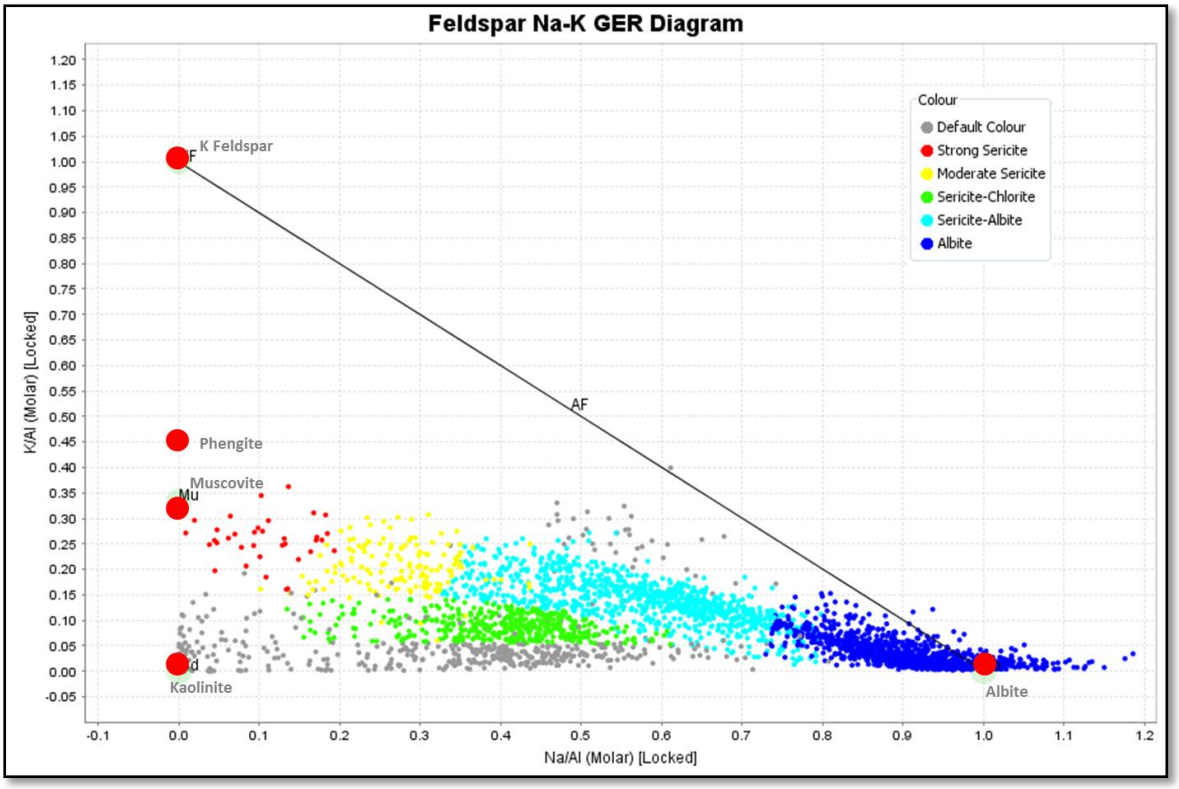

Fig. 4.9 Molar K-Al-Na ratio plot identifying the projected alteration signatures of all rocks with the help of element ratio tie lines.

This alteration classification when plotted as a cross section shows a strong correlation between intense albite alteration and gold. The intense albite alteration extends for about 100 m into the footwall (Figs. 4.10a and 4.10b).

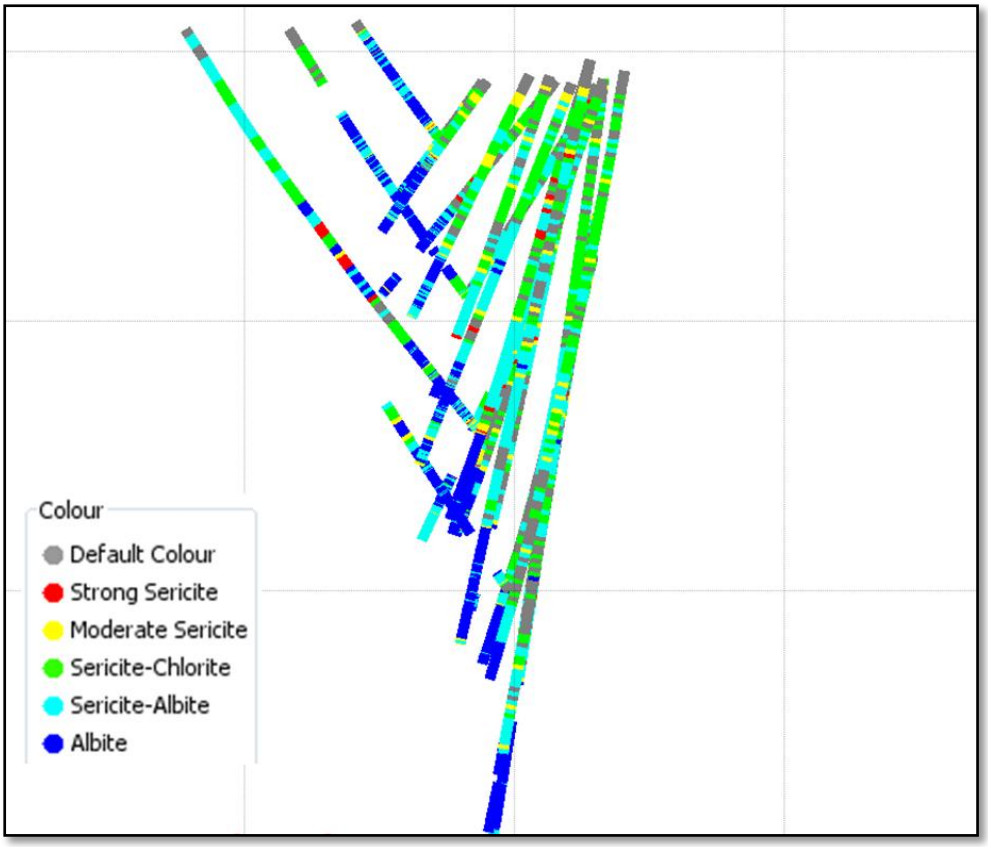

Fig. 4.10a Alteration mineralogy determined from the lithogeochemistry plotted as a cross section (section looking north).

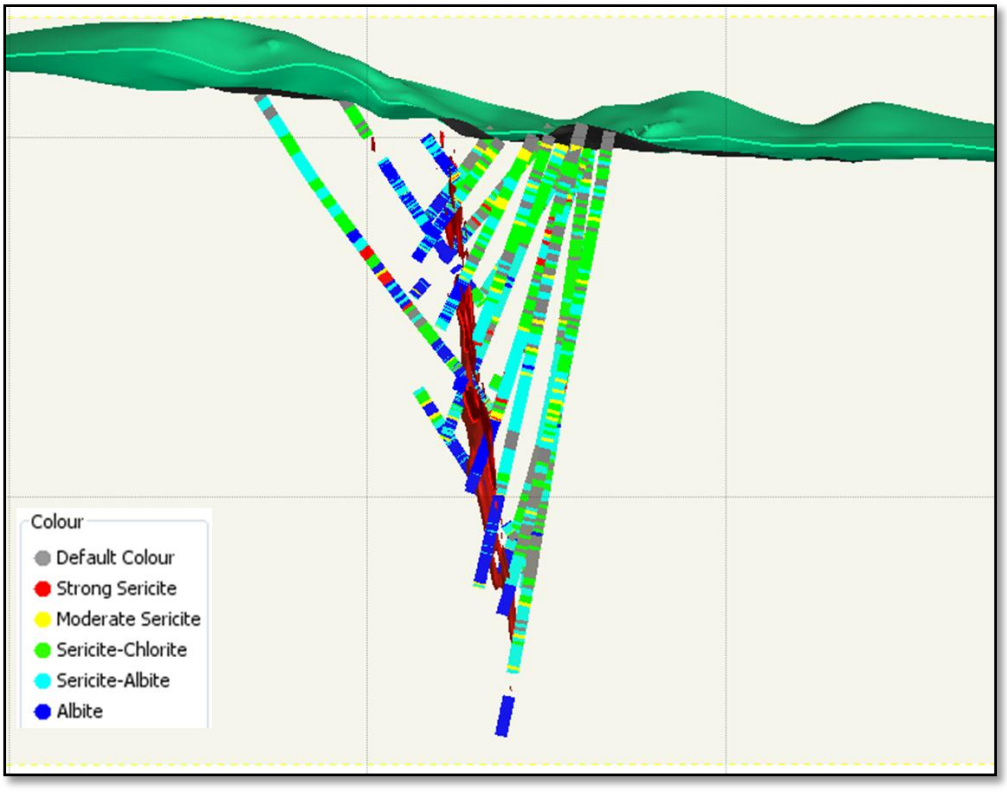

Fig. 4.10b Mineralogy section plotted in leapfrog software with a 2.0g/t grade shell in red.

4.2.2 Carbonate Composition Ca-Fe-Mg Ternary Plot

Ternary diagrams are frequently used in geochemistry for resuming and inspecting in geological samples the abundance of three selected components (or end-members) in a bi-dimensional space (Halley, 2011). In this case the composition of carbonate (dolomite-ankerite) in relation to Ca-Fe-Mg.

In the Ca-Fe-Mg ternary plot in Figure 4.11, all the most intensely altered samples (i.e. the strongly albite altered samples) project back to a single point on the dolomite-ankerite tie line. It is clear that the cluster of points form a trend between Fe corner (pyrite) and a point mid-way between dolomite and ankerite. This indicates that the carbonates are all the same composition and most of the carbonate occurs with albite. All of the albite altered samples plot as a linear trend between ferroan carbonate and pyrite (Fig. 4.12). The weak sericite group (green) is mostly on the Mg-rich side of the carbonate-pyrite trend. These points will actually be mixtures of sericite and chlorite.

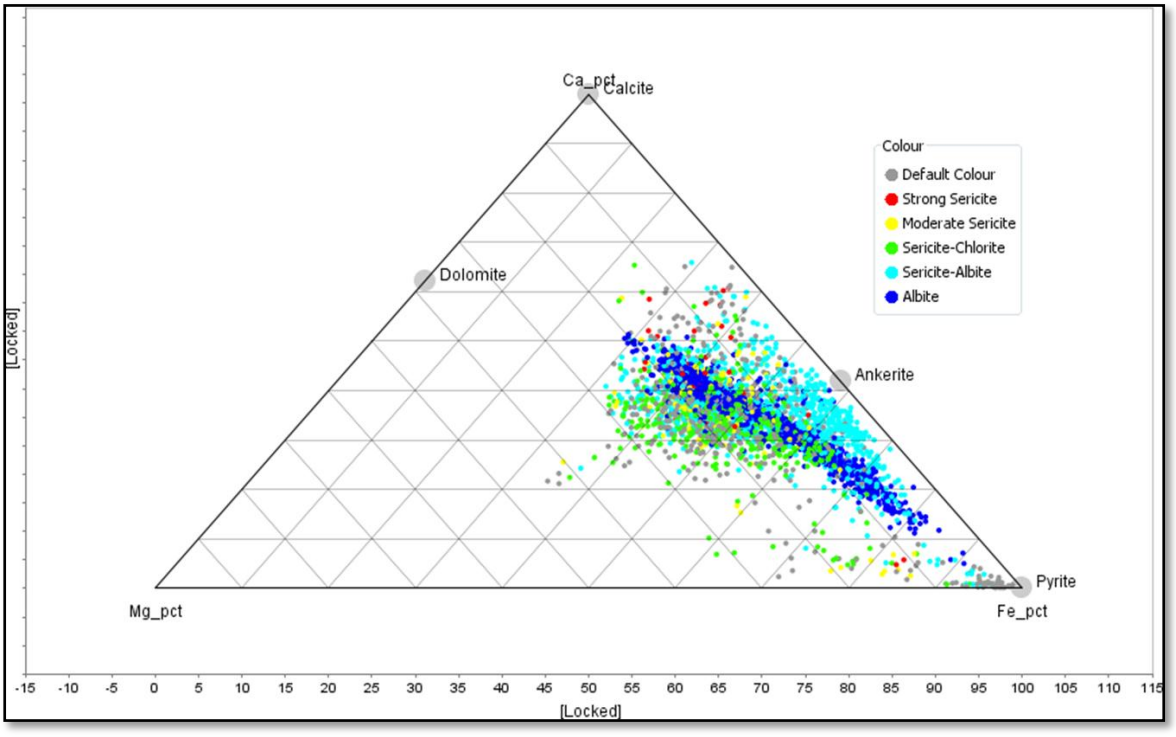

Fig. 4.11 Molar Ca-Fe-Mg ternary plots for alterations.

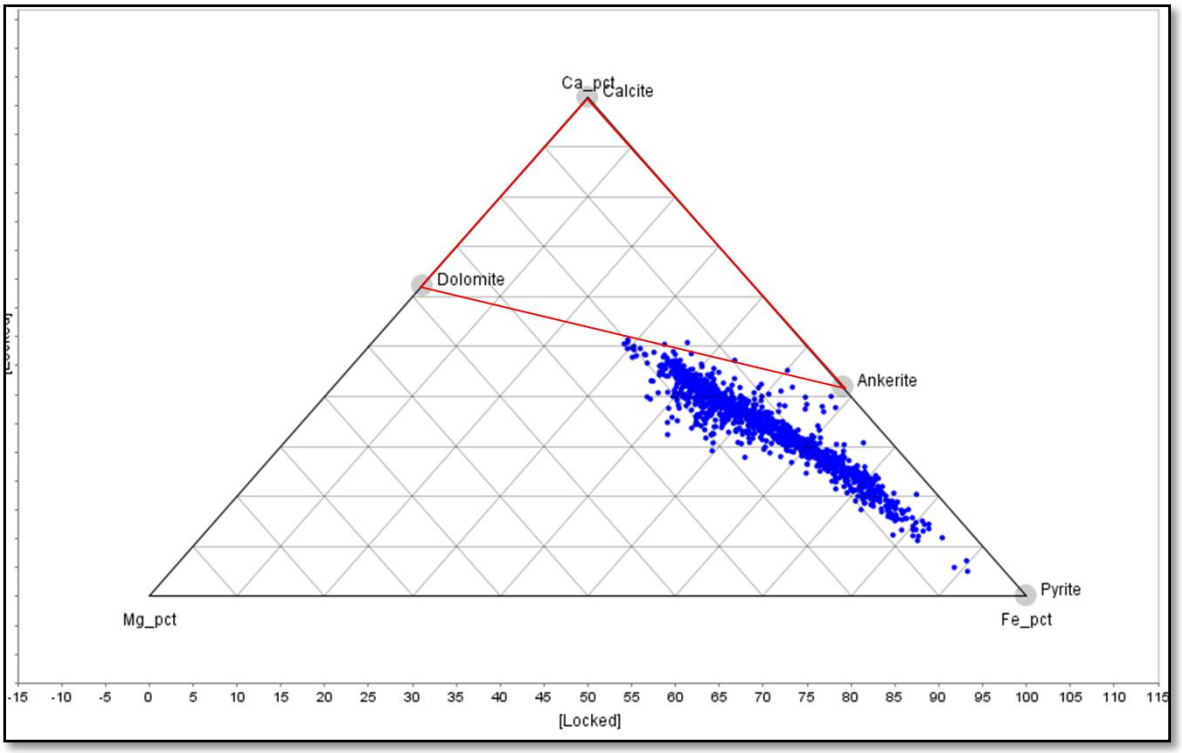

Fig. 4.12 Molar Ca-Fe-Mg ternary plot for albite alteration.

4.3 ASD Alteration Mineralogy

4.3.1 Feldspar-Sericite K/Al vs Na/Al Molar Ratio Plot

One way to quantify the chemical changes during alteration is to plot the whole rock analysis as general element ratios of Potassium/Aluminium (K/Al) versus Sodium/Aluminium (Na/Al). In this way, the relative amount of sericite or albite can be quantified. In Figure 4.13 plot, the geochemical assay points are coloured by the mineralogy mapped with the ASD. It shows the correlation between mineralogy from lithogeochemistry and the ASD. The ASD cannot measure albite; the assay method used here does not also measure carbonate. However, when the geochemistry results are coloured using the ASD mineralogy the correlation between carbonate and albite is very clear. All the points plotting on the join between albite and muscovite are either carbonate or sericite. Below this join, the ASD is measuring sericite+chlorite or chlorite.

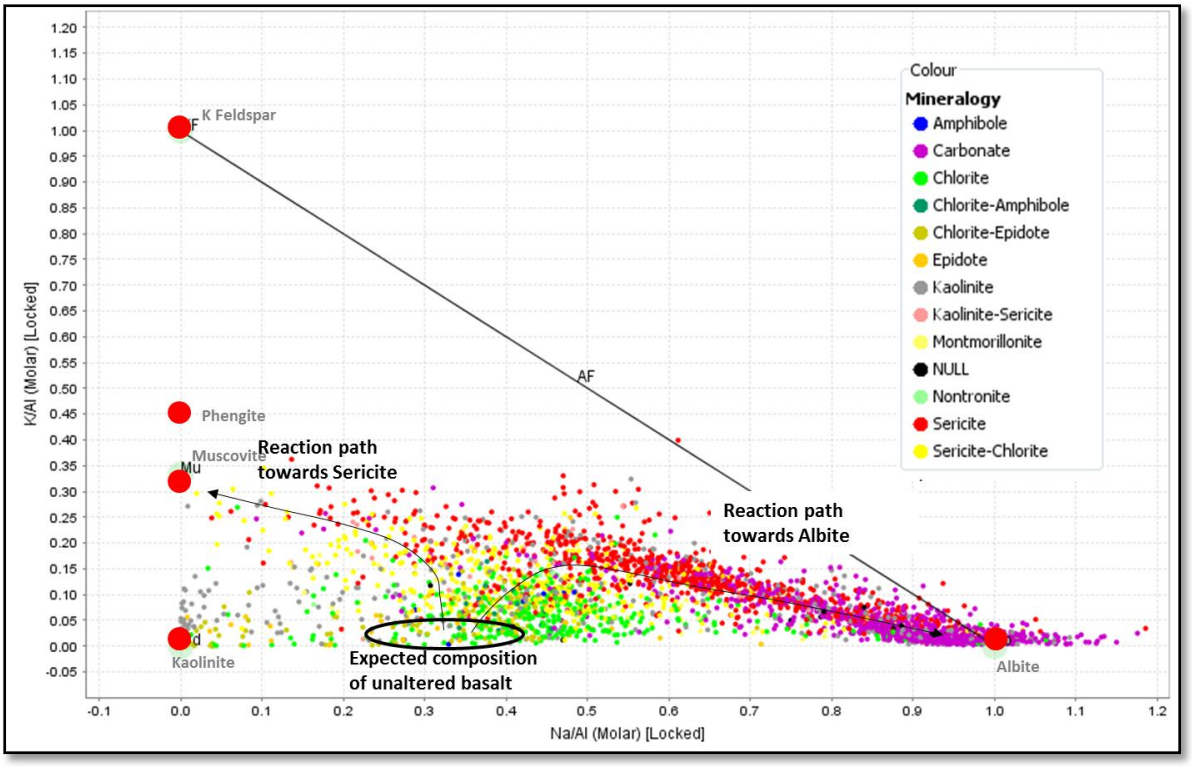

Fig. 4.13 Feldspar-Sericite K/Al versus Na/Al molar ratio plot coloured by ASD mineralogy.

The ASD mineralogy when plotted on the same section as the lithogeochemistry in Figure 4.10a shows a strong correlation between carbonate measured with the TerraSpec and albite measured from the geochemistry (Fig. 4.14). The TerraSpec cannot measure albite content, but it is clear in Figure 4.14 that the albite-carbonate defines the proximal alteration assemblages. This is surrounded by a distal halo of sericite-chlorite and other minor alteration minerals such as epidote and montmorillonite.

Figure 4.15 is a modelled shape of the carbonate alteration from the ASD results as a 3D volume, shown in purple and the albite alteration from the multielement geochemistry is also shown as a 3D volume in light blue. These are plotted on a 3D slice with gold grades, blue <0.2 ppm, red >2 ppm. The carbonate alteration exactly defines the ore zone whilst the albite alteration slightly extends into the footwall.

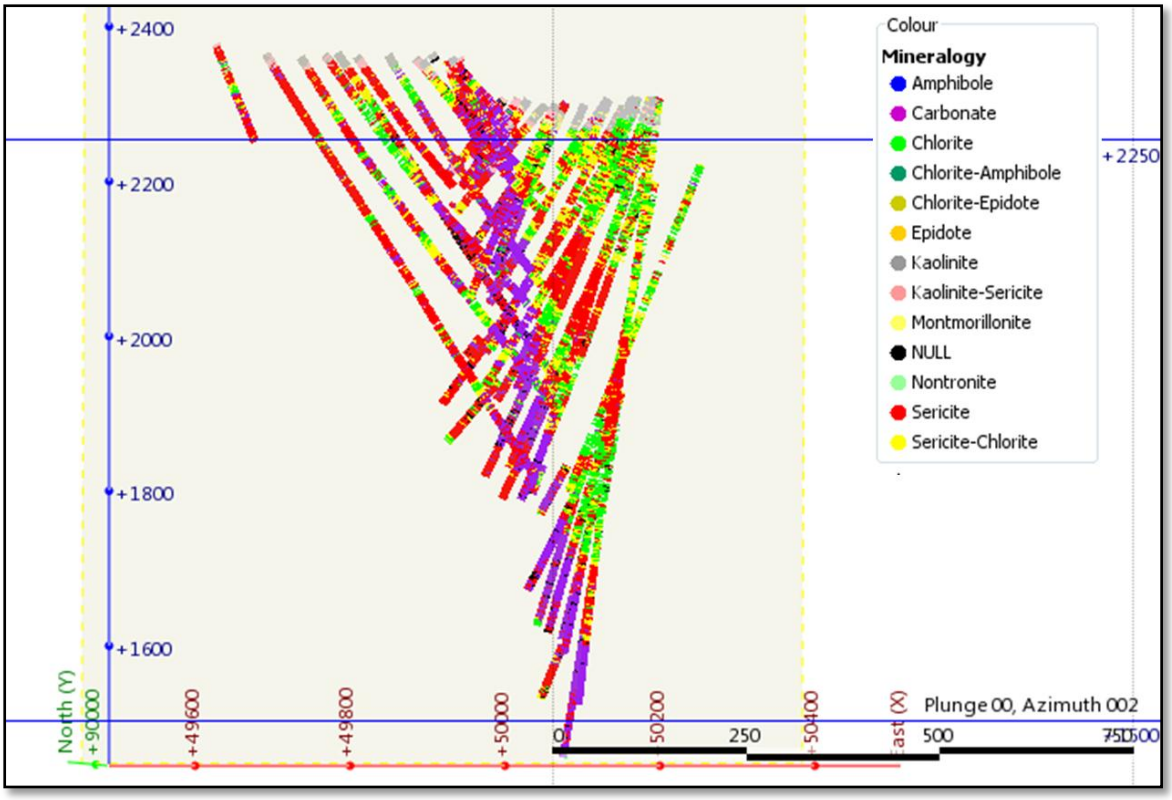

Fig. 4.14 ASD mineralogy section (section looking north).

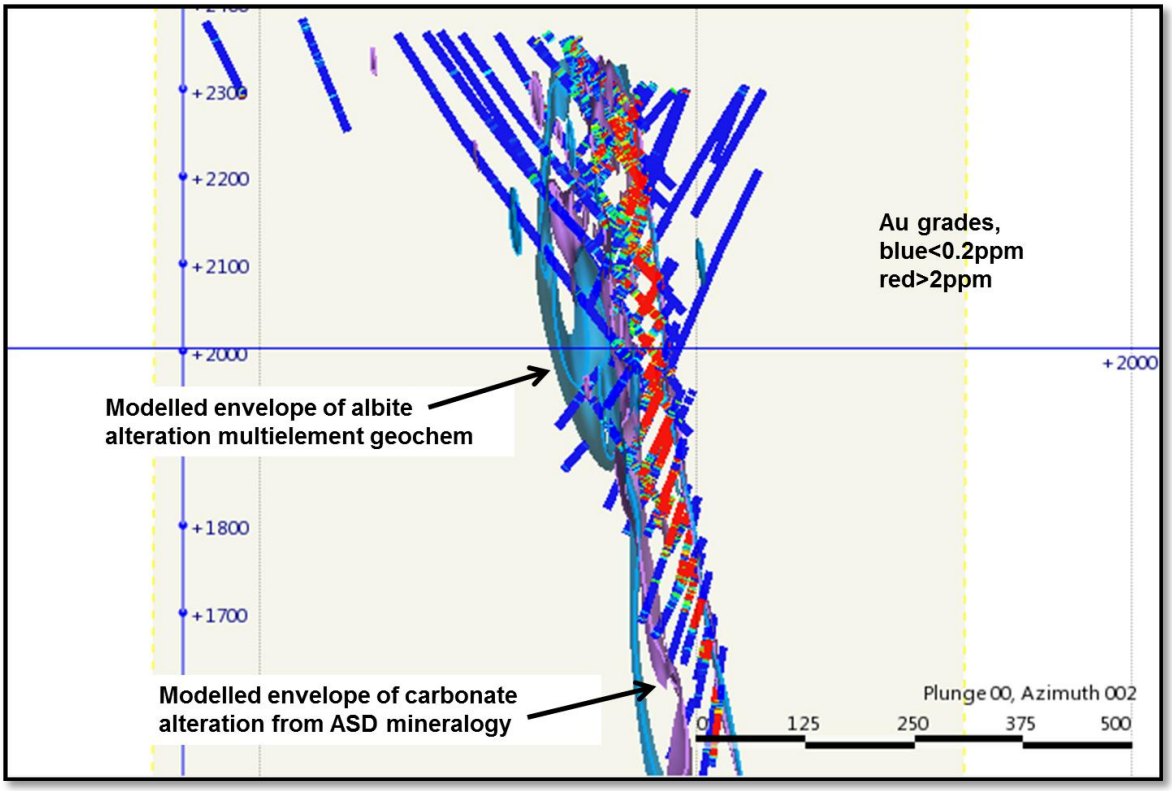

Fig. 4.15 Carbonate and albite alteration model (section looking north).

4.3.2 ASD Carbonate Composition Ca-Fe-Mg Ternary Plot

On the Ca-Fe-Mg ternary plot, all the intensely altered carbonate samples project back to a single point on the dolomite-ankerite tie line (Fig. 4.16). This indicates that the carbonates are all the same composition and that composition is midway between ankerite and dolomite. All of the carbonate-rich ASD results plot as a linear trend between ferroan carbonate and pyrite.

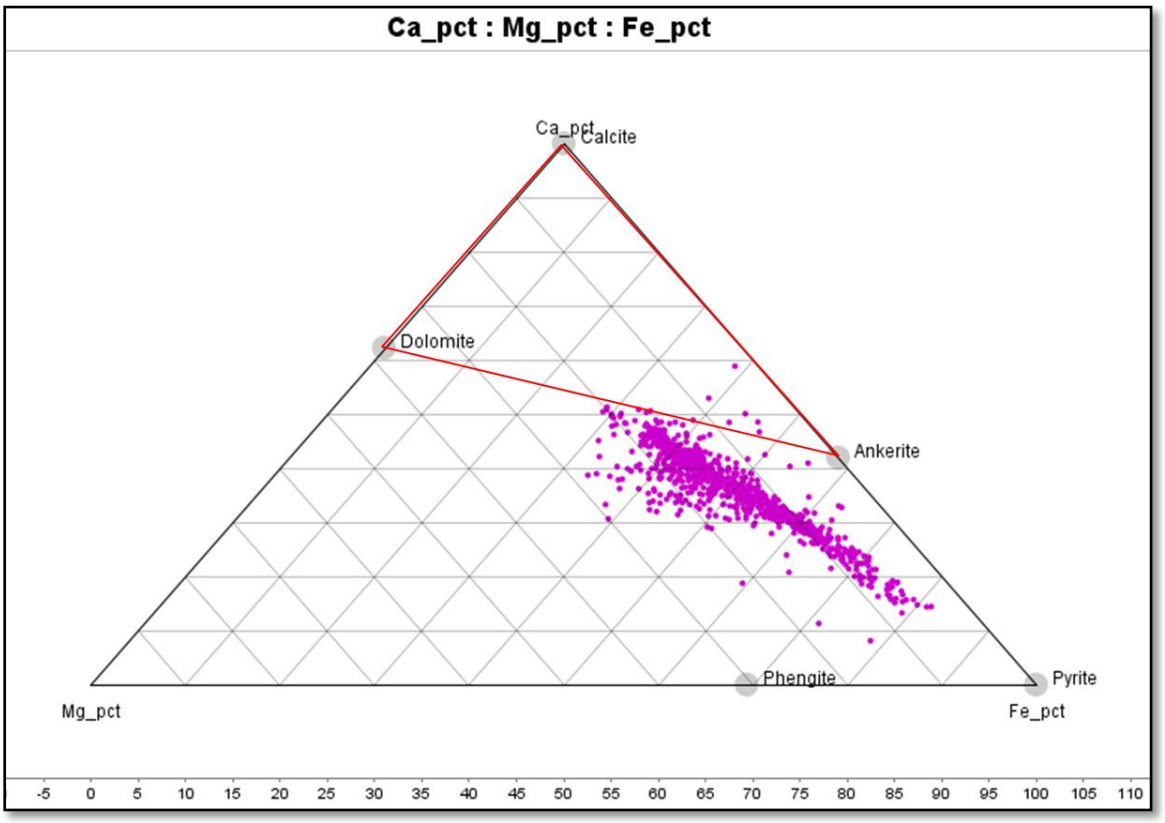

Fig. 4.16 Ca-Fe-Mg ternary plots for carbonate alteration.

4.3.3 ASD Sericite Chemistry

Every spectrum where sericite was recorded, the wavelength of around the 2200 nm feature was selected. Figure 4.17 shows a section looking north showing the sericite wavelengths of around 2200 nm; blue<2205 nm, red>2218 nm. There is a contrast between very long and very short wavelengths across the orebody.

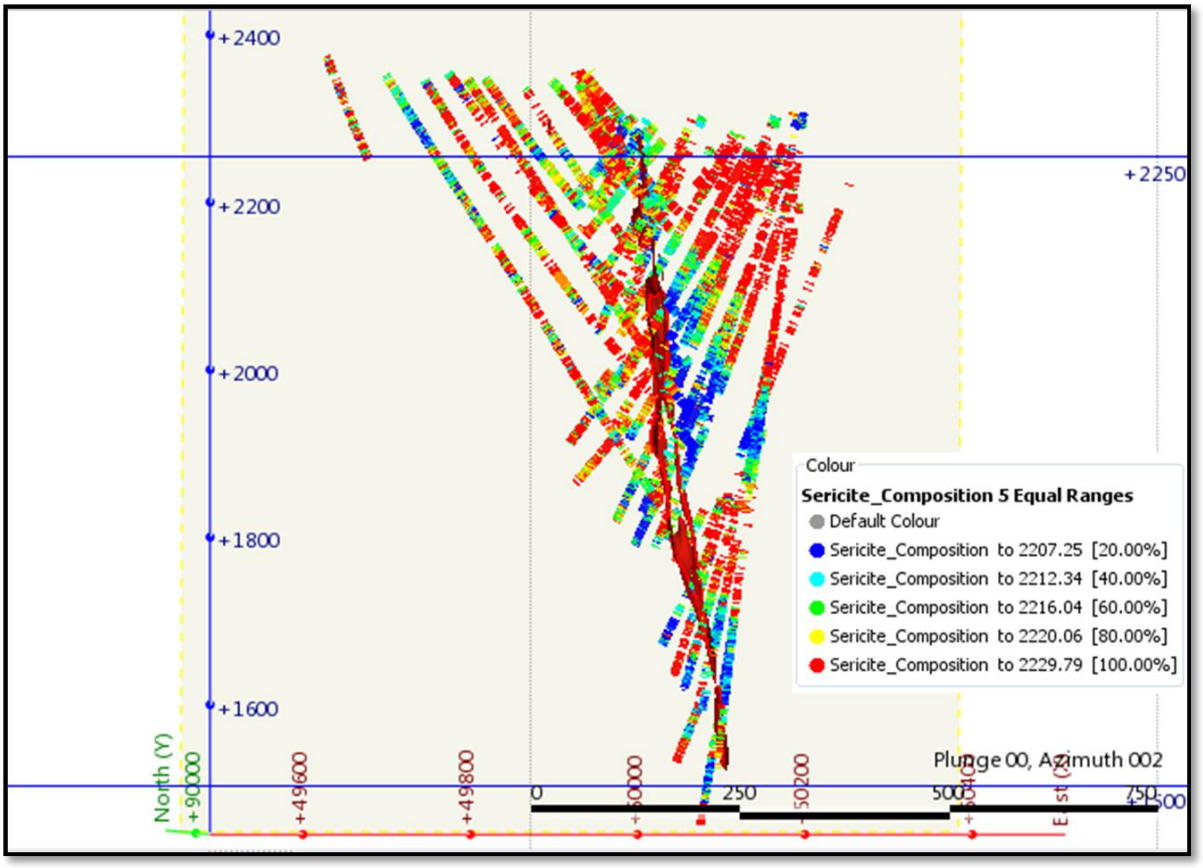

Fig. 4.17 A plot of ASD sericite composition on a section (section looking north).

The plot in Figure 4.18 is a level plan of a horizontal slice through the center of the high grade core in Paboase. There is a contrast between very long wavelength sericite in the hangingwall and very short wavelength sericite in the footwall. The highest gold grades occur with albite and carbonate. Au occurs with intermediate wavelength sericite rather than very long or very short wavelengths.

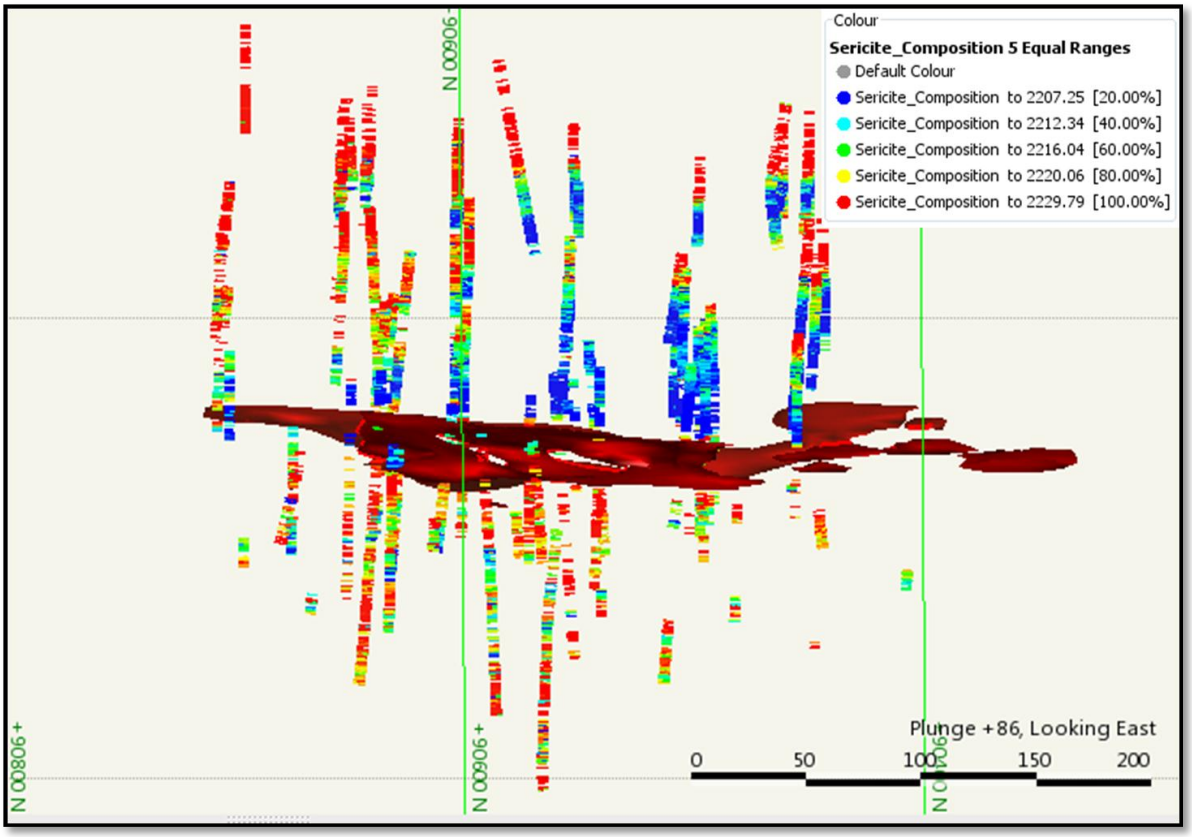

Fig. 4.18 A level plan showing the different sericite wavelengths.

4.4 Pathfinder Signatures

4.4.1 Pathfinder Element Distribution – Geochemistry

Probability plots show how pathfinder metal distributions are correlated with alteration mineralogy (Halley, 2011). Anomalous pathfinder element values are controlled by host rock mineralogy; therefore, if they are correlated with the dominant silicate mineral assemblages identified in the molar abundance plots they can act as a relative proxy for the assemblage distribution and may identify deposit-and even district-scale geochemical halos that can be utilized in exploration. Each pathfinder is plotted against the N-Score that is derived by a formula. N-score is the (assay – median) / standard deviation. The median assay value will have an N-score of zero. An element with a normal distribution will plot as a reasonably straight line. An anomalous population will plot as an upward inflection on the probability curve at the high-end values (Halley, 2011).

Figure 4.20 shows that the least altered rocks have the highest arsenic contents. The average crustal abundance of arsenic is around 5 ppm (Halley, 2011). The least altered rocks are around that level. The albitised rocks are depleted in arsenic. It is quite rare in hydrothermal systems to unequivocally demonstrate the depletion of a chalcophile element. The most arsenic depleted rocks are the low grade carbonate-albite altered rocks on the margins of the ore zones. These are the zones where hydrothermal hematite is most abundant. That is, arsenic is most clearly depleted in the most oxidized hydrothermal assemblages (Halley, 2011). The average crustal abundance of antimony is around 1 ppm (Halley, 2011). There is surprisingly little variation in antimony content from one alteration style to another. There is insignificant addition of Sb within this system.

Sulfur (pyrite) is clearly most abundant in the albite-carbonate assemblage. Within this assemblage, the median S value is 0.25%, which equates to 0.5% pyrite. Lithium substitutes for Mg in Fe-Mg minerals. It is common to see Li enrichment as an outer halo around hydrothermal systems. In this case however, the sericite and albite rich alterations do not accommodate Li and there is widespread Li depletion (Fig. 4.20). The albite zones contain much higher bismuth and tellurium values than the other alteration assemblages. However, the absolute values of Bi and Te are not that high, and they are spatially restricted.

Gold is very strongly biased towards the albite-rich rocks. Molybdenum is highly anomalous in this system, but with an even more restricted distribution than gold (steeper tail on the probability plot). The tungsten values are moderately anomalous, but very consistently anomalous across a range of alteration types. All of the albitised alteration is anomalous in tungsten, and the W extends into more moderate alteration zones as well.

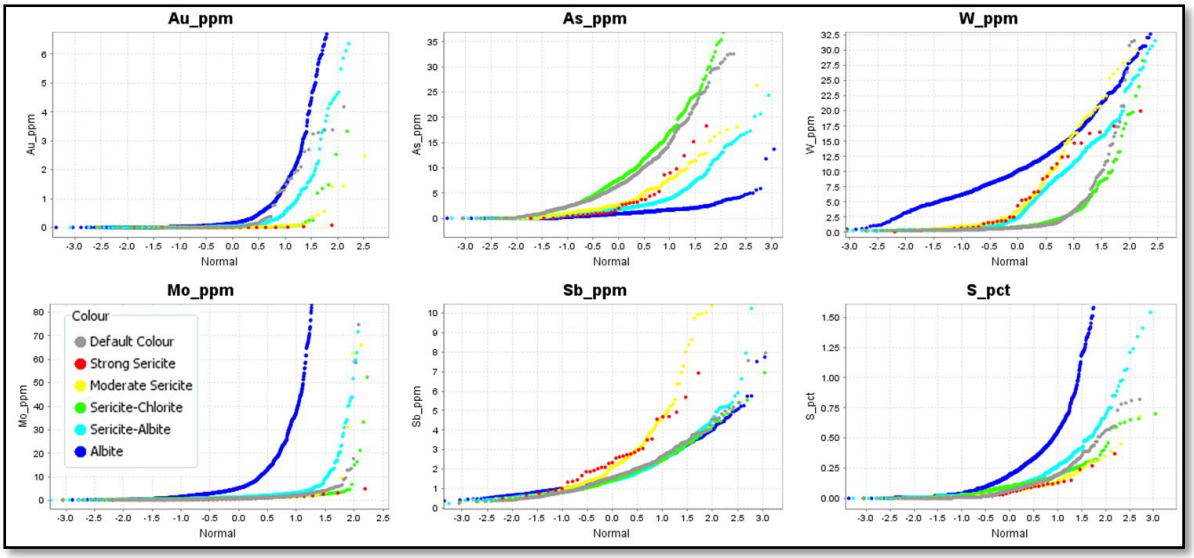

Fig. 4.19 Probability plots based on the N-Score distribution of pathfinder element; gold, arsenic, tungsten, molybdenum, antimony and sulphur split by alteration types.

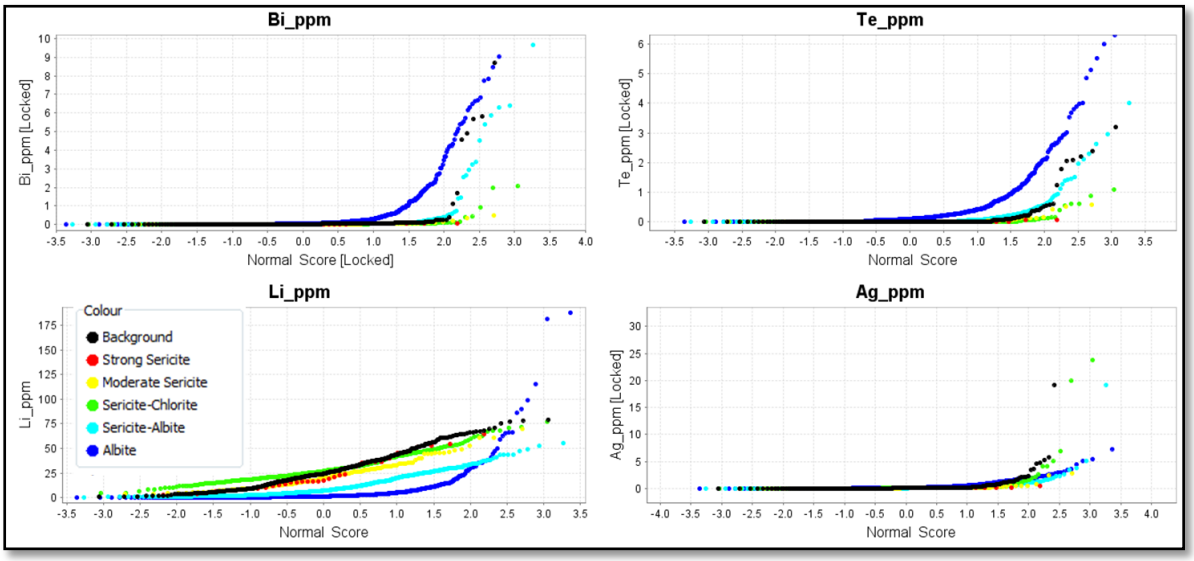

Fig. 4.20 Probability plots based on the N-Score distribution of pathfinder element; bismuth, tellurium, lithium and silver split by alteration types.

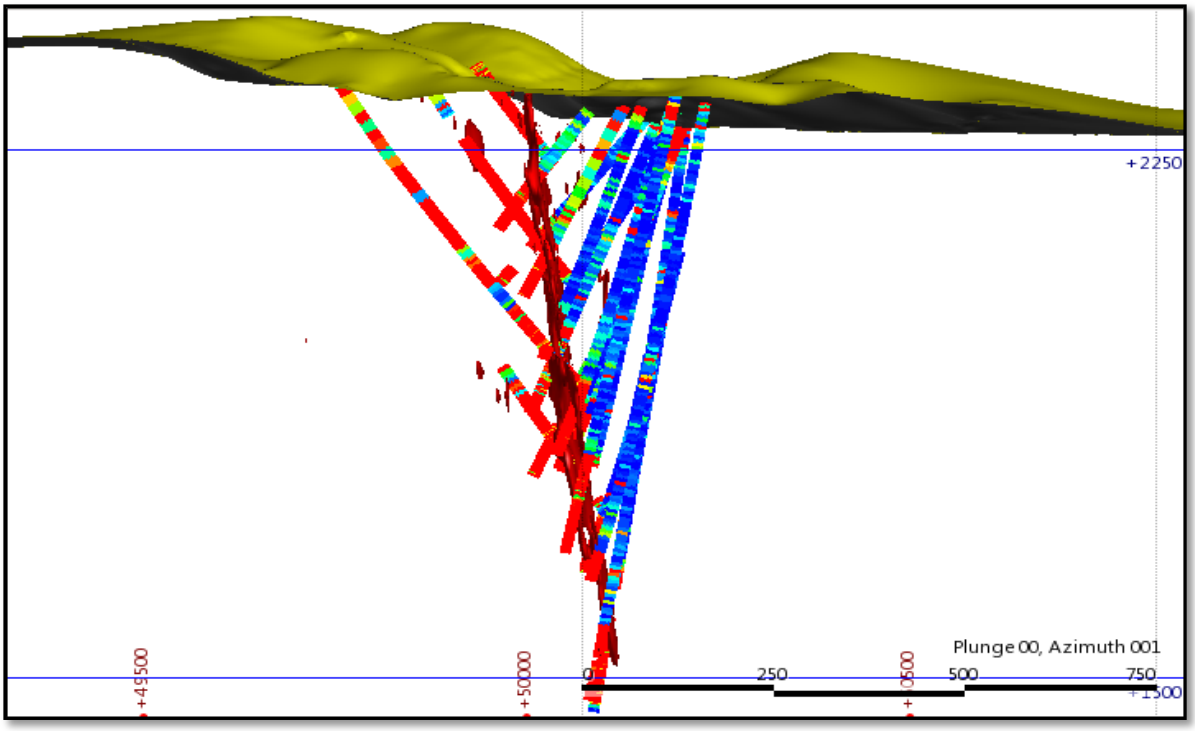

Fig. 4.21 A model of a section looking north of tungsten grades.

Figure 4.21 shows the same view as the alteration mineralogy in Figure 4.10b above, showing Tungsten assays; blue<0.5 ppm, red>5 ppm. The tungsten extends a long way into the footwall. Within the intensely albite-altered rocks, W is consistently anomalous, and it plots as a single population with exceptionally low variance. To have a pattern like this, it must be hosted in a very broadly distributed mineral, rather than occurring in scheelite. The mineralogy of the proximal alteration zone is albite-pyrite-carbonate. The tungsten must be hosted in one of these minerals. The plots in Figure 4.22 show the relationship between tungsten and gold, sulfur (pyrite), sodium (albite) and magnesium (ferroan dolomite). Although W and Au broadly occur in the same zone, they are not correlated at all. There is no correlation with pyrite content (S) or carbonate content (Mg in ferroan dolomite). All of the albite rich rocks have 5 ppm to 20 ppm W. This strongly suggests that trace amounts of W are hosted within the lattice of albite. If this knowledge is transferred to a soil sampling program, it could now infer that W in soils will be a proxy for mapping albite haloes in the underlying bedrock.

4.4.2 Probability Plots of Pathfinders coloured by ASD Mineralogy

The probability plots in Figure 4.24 are coloured by ASD mineralogy. Gold is very strongly biased towards the carbonate-rich rocks. Tungsten is uniformly elevated in the carbonate-rich rocks, but also shows high values in the adjacent sericite-rich and even chlorite-rich rocks. Molybdenum is strongly skewed towards the carbonate-rich alteration. The probability plot for sulfur shows that the carbonate-rich zones are significantly more pyrite-rich. Arsenic is depleted in the sericite and carbonate zones.

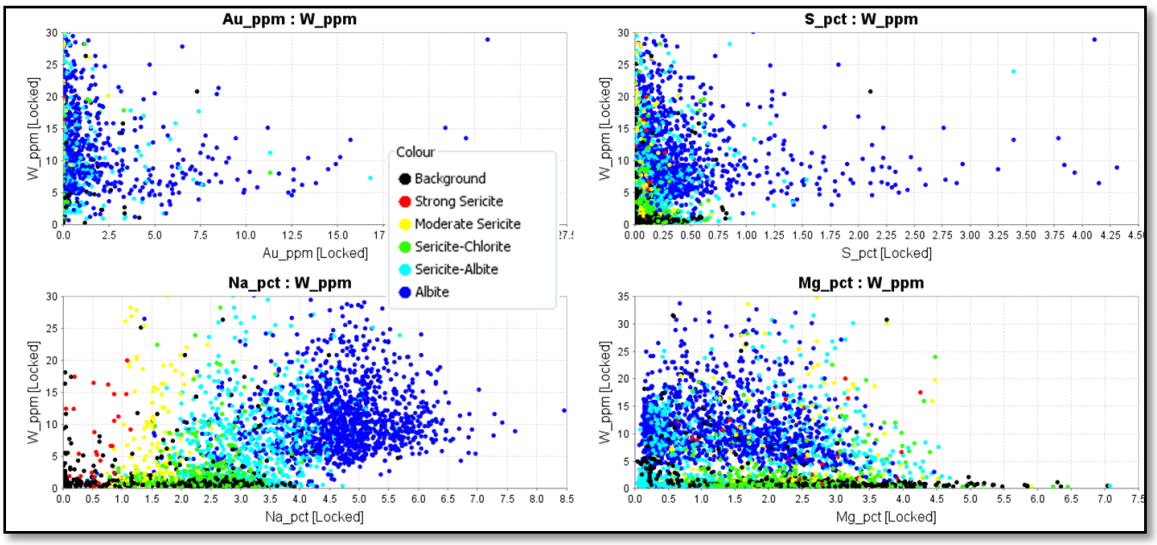

Fig. 4.22 Scatter plots of Tungsten against Au, S, Na and Mg.

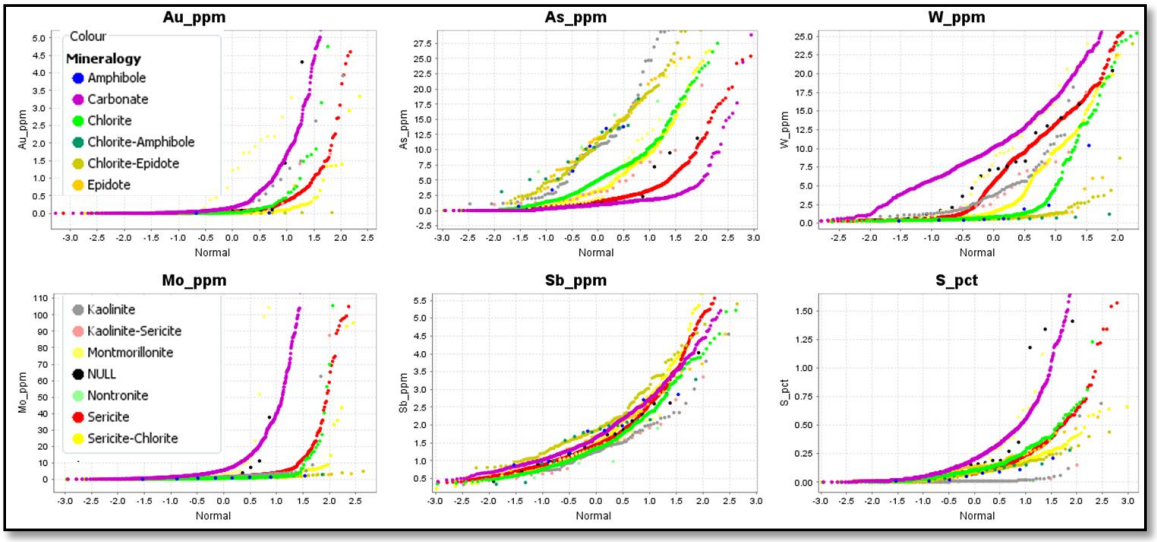

Fig. 4.23 Probability plots of pathfinder elements by ASD mineralogy.

CHAPTER FIVE

DISCUSSION

Paboase is associated with porphyry intrusions with albite-dolomite-pyrite alterations. Gold mineralization is largely hosted in altered mafics (quartz dolerite) and porphyry intrusive rocks (Fig. 5.1). The association of hematite-magnetite-pyrite in the porphyries and mafic host rocks indicates a much oxidized hydrothermal system. Graphite is present in quartz breccias with pyrite, commonly with stylolitic textures in zones of strongly elevated gold mineralization. The graphite indicates a change to much reduced hydrothermal conditions later in the paragenesis. Although high grade gold is associated with black breccias, the critical thing is the amount of pyrite and not the amount of quartz. It was formally thought the black breccia contain high amount of graphite but LECO (Laboratory Equipment Corporation) results for the graphitic samples revealed that the samples have much lower graphite contents than originally assumed (Smeathers, 2009).

The scandium scatterplots distinguished between the mafic and felsic compositions of the highly altered host rocks. In addition, the Sc vs. Ti scatterplot is of particular use in the identification of a different mafic unit that has high Ti content which was identified as small, late, cross-cutting dyke whereas Sc vs. V, and Zr plots which has low V and high Zr distinguished different felsic intrusion units. The molar ternary and molar ratio plots defined igneous compositional changes and the effects of superposed hydrothermal alteration. The molar-based classification alteration mineral types generated alteration haloes of the mineral assemblages. In turn, these provide information on the alteration haloes and hydrothermal fluid dispersion patterns that may aid in exploration.

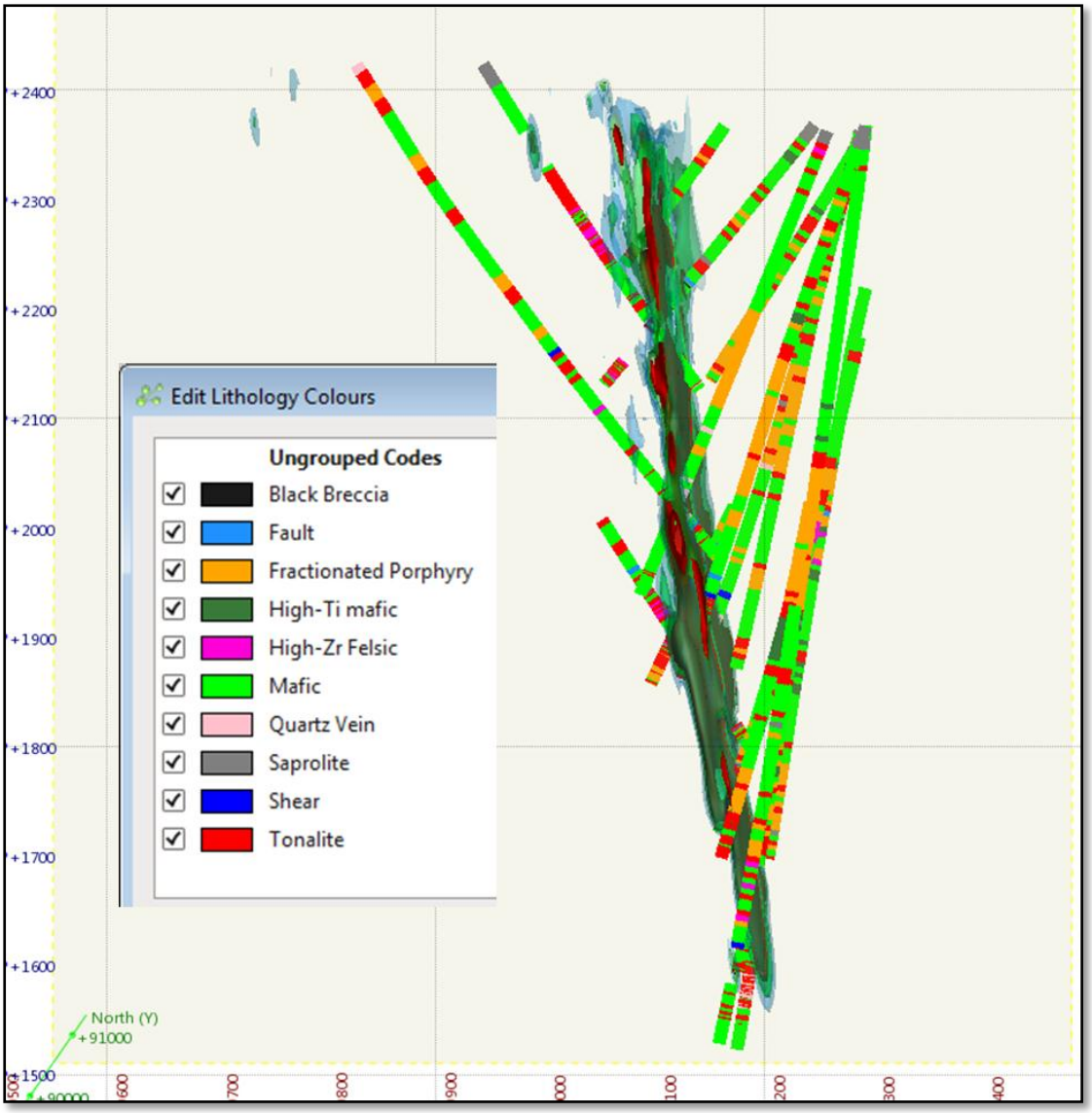

Fig. 5.1 Paboase lithogeochemical cross section with gold grade >0.5g/t.

The multielment geochemistry shows a quite weak fractionation trend among the mafic rocks, despite the doleritic and gabbroic textures. One different exotic mafic dyke signature can be recognised. Amongst the porphyries, two different compositional groups were recognized. There is a small scale intermixing of felsic dykes within mafic volcanics. It has been suggested by some observers that the felsic dykes may be the end product of fractionation from the same magma chamber as the mafic volcanic (Halley, 2011). Halley

noted that the mafic volcanics and porphyry intrusions all plot on the same fractionation path and that does not rule out a genetic link.

Within the area sampled in this study, virtually all of the basalts are altered to some extent. Relict amphibole is very rare. In contrast, alteration on the Ekyuiabo, one of the deposits at Chirano which is located along the Bibiani shear in the sedimentary basin is intensely sericitic. There is no relict feldspar. Some of the sericite is an ammonium-bearing variety, including the sericite in the mineralized porphyry at Bibiani. The ammonia is likely to be derived from the organic material in the Birimian sediments (Halley, 2011).

The dominant alteration signature in the ore zone mapped by the geochemistry is albitisation (Fig. 4.11b) along with ferroan dolomite and pyrite. This is surrounded by sericite-albite, then sericite-chlorite and distal chlorite. In a large percentage of the samples, the albitisation process has gone to completion. All of the available Na and Al in the rock are contained in albite.

The Paboase sections are characterized by a very broad range of white mica compositions. In the Short Wave Infrared data, the broad range of mica compositions is demonstrated by a complete range of very long to very short wavelengths of the Al-OH absorption features associated with the white micas. Au occurs with intermediate wavelength sericite rather than very long or very short wavelengths. The ASD mineralogy plotted on the same section as the lithogeochemsitry (Figs. 4.10a and 4.10b) shows a strong correlation between carbonate measured with the TerraSpec and albite measured from the geochemistry (Fig. 4.14). There is a 150 m wide zone where the ASD maps strong carbonate alteration. It is evident in Figures 4.10a and 4.14 that the albite-carbonate defines the proximal alteration assemblages. This is

surrounded by a distal halo of sericite-chlorite and other minor alteration minerals such as epidote and montmorillonite.

Paboase has a W-Mo-Bi-Te signature. This is in contrast to the typical Birimian gold deposit signature of K, As, Fe and Sb, Leube et al., (1990). The K, As, Fe and Sb suite of elements is depleted in the albite alteration zones that correlates very well with gold at Paboase (Figs. 4.20 and 5.2). In addition, these elements are not correlated with the strong carbonate alteration mapped by the ASD which forms a halo around the gold lodes (Figs. 4.24 and 5.3). However, the Ekyuabo deposit in the sedimentary basin does contain the typical As-Sb pathfinder signatures (Halley, 2011).

The Mo-Bi and Te have a strongly skewed distribution, and they are highly correlated with gold, so their usefulness as pathfinders is limited. A pathfinder element that is highly correlated with gold is not particularly useful, we may as well assay for gold. For a pathfinder element to be useful, it should have a much lower nugget affect than gold. If a sample is taken from within the mineralized system, it should always return a relatively high value and not have a hit or miss nugget response. Secondly, the pathfinder should have a much broader distribution than gold, so that beyond the ore zone, it drops off to background levels gradually rather than rapidly. Tungsten is remarkably uniformly distributed in the albite-dolomite rocks, and has a halo extending far beyond the footprint of the gold. The albitised alteration rocks are anomalous in tungsten and the tungsten extends into more moderate alteration zones as well (Fig. 4.19).

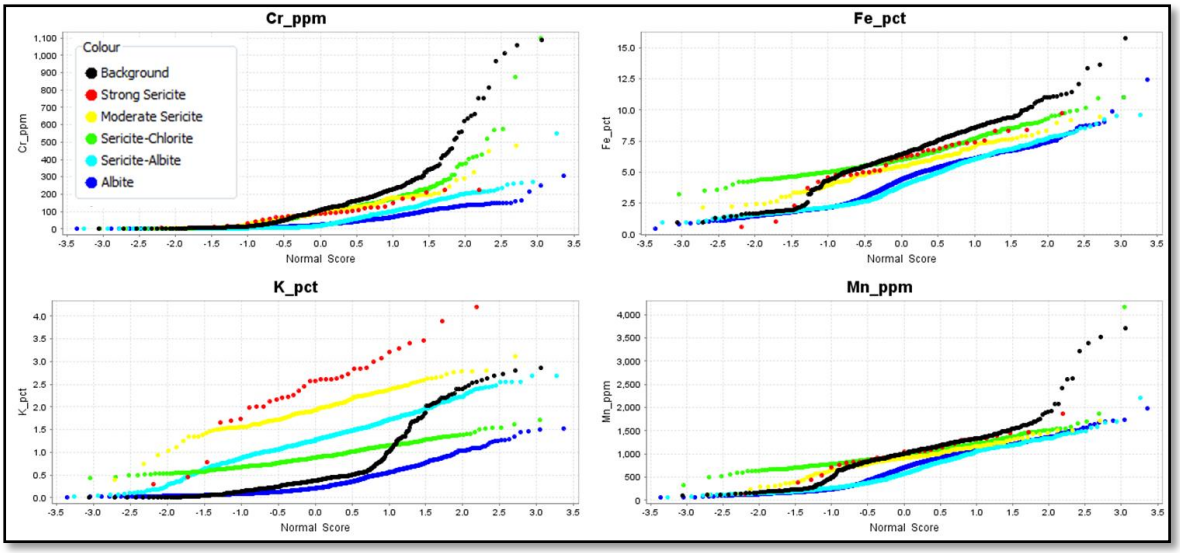

Fig. 5.2 Probability plots of chromium, iron, potassium and manganese split by alteration types.

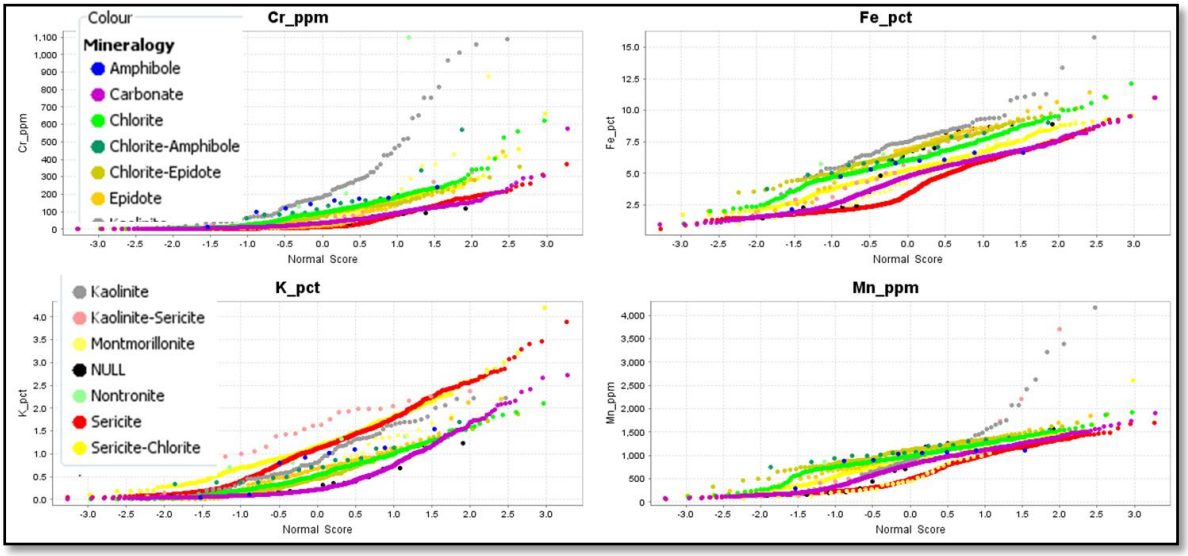

Fig. 5.3 Probability plots of chromium, iron, potassium and manganese split by ASD alteration types.

Arsenic is clearly depleted in the proximal parts of the system. Arsenic is soluble in oxidized hydrothermal systems so the depletion is as result of flushing the rocks with an oxidized fluid early in the history of the system. Also, low arsenic values as a whole possibly indicate regional depletions when compared to pelitic sedimentary hosted graphitic shear zones of the Ashanti and Bogoso deposits in Ghana. These deposits subject to arsenic input from the surrounding sediments contrast with Chirano where only the Akwaaba deposit is associated with Tarkwaian sediments (Allibone et al., 2004). It is noted by Roberts (2010) that Akwaaba

shows enrichment in As compared to Paboase. This difference can be attributed to arsenic leaching into the Akwaaba mafics through the dividing Chirano shear zone as all high values are contained nearest the shear zone.

At Paboase, gold and sulphur are highly correlated with the albite and carbonate alterations in the same zone (Figs. 4.20 and 4.24). The reduction reaction that precipitates pyrite also causes gold to deposit. Stable isotope analyses by Smeathers (2009) show that the early formed pyrite precipitated from sulfate-rich fluids and the fluid inclusions in the quartz have a very high proportion of methane. This progression from early oxidized to late reduced signatures is another common feature of Archean gold systems (Halley, 2009). Gold precipitates in response to a gradient in fluid chemistry; if the chemistry of the fluid doesn't change, metal will not precipitate. The switch from oxidized to reduced is the trigger for dropping out gold (Halley, 2011).

The pathfinder associations described above all have redox sensitive solubility products. Antimony and arsenic are proxies for mapping where the hydrothermal systems have become reduced (Halley, 2009). These metals are more soluble in oxidized environments, and precipitate in reduced environments (Halley, 2011). The position where they occur in a hydrothermal system is governed by the oxidation state and temperature of the system. The zonation will be from Mo → Bi → As → Sb as a system evolves from hot and oxidised to cool and reduced (Halley, 2009). The sedimentary environment having arsenic and antimony footprints suggests that the sedimentary environment indicates a more reduced environment as compared to the volcanic environment where Paboase is located which indicate a more oxidised environment in the early part of the system. Therefore the pathfinder signature of

these types of deposits is vastly different when they are within or juxtaposed next to the sediments.

The major findings of this research are summarized below;

- Gold mineralization in Paboase is hosted in mafic and porphyry intrusive rocks.
- Two different compositional groups were identified among the porphyries; one that have low V relative to Sc, while the other Zr -rich.
- The fine grained and coarse grained mafic rocks are geochemically identical.
- The proximal alteration is carbonate-albite-pyrite and this is surrounded by a distal halo of sericite-chlorite.
- Within the porphyries, the mineralogy is sericite-rich and sericite-chlorite alteration is very widespread in the mafic rocks.
- Paboase has a Tungsten-Molybdenum-Bismuth-Terrarium (W-Mo-Bi-Te) pathfinder signature, but tungsten is the best pathfinder for gold
- The trace amounts of W are hosted within the lattice of albite, for which reason W in soils could be a proxy for mapping albite haloes in the underlying bedrock.

CHAPTER SIX

CONCLUSION

Gold mineralization is largely hosted in altered mafics (quartz dolerite) and porphyry intrusive rocks. This is in sharp contrast to Allibone et al. (2004) who stated that economically significant mineralization at Chirano is largely hosted by altered tonalite intrusions.

The proximal alteration is carbonate-albite-pyrite (Figs. 4.11b, 4.14, 4.15, and 4.16). This is surrounded by a distal halo of sericite-chlorite. Within the porphyries, the mineralogy is sericite-albite-rich with minor chlorite. Sericite-chlorite alteration is very widespread in the mafic rocks. Sericite cannot form in mafic rocks without potassium metasomatism.

Pathfinder elements are strongly controlled by host rock mineralogy; therefore, if they are correlated with the dominant silicate mineral assemblages identified in the molar abundance plots, they can act as relative proxy for the assemblage distribution and may identify deposit- and even district-scale geochemical haloes that can be utilized in exploration. In the case of Paboase four pathfinder elements were identified, W, Bi, Te and Mo. However, comparing the probability plot profiles of W to those of Mo, Bi and Te, particularly for albite and carbonate rich rocks that correlates very well with Au, Mo, Bi and Te have a flat zone on the probability profile with a sharp upward inflection defining a small anomalous population. Tungsten is remarkably uniformly distributed in the albite-dolomite rocks, and has a halo extending far beyond the footprint of the gold. Tungsten is therefore the best pathfinder for gold at Paboase.

The host rocks for the anomalous W are essentially just albite-pyrite-dolomite rocks. At Paboase, W is highly correlated with albite alteration. The W has very low variance, so it cannot be hosted in scheelite. Probability plots of tungsten against S (pyrite), Mg (dolomite) and Na (albite) suggest that albite is the host for the anomalous W. At surface, albite will be converted to kaolinite (Halley, 2011). Measuring W in the soil geochemistry will now be a proxy for mapping the width of the albite alteration halo.

REFERENCES

Actlabs, (2013). Lithogeochemistry for Research and Mineral Exploration: Available at (http://www.activationlabs.com/files/Lithogeochemistry.pdf)

Allibone, A., Teasdale, J., Cameron, G., Etheridge, M., Uttley, P., Soboh, A., Appiah-Kubi, J., Adanu, A., Arthur, R., Mamphey, J., Odoom, B., Zuta, J., Tsikata, A., Pataye, F., Famiyeh, S., and Lamb, E. (2002). Timing and Structural Controls on Gold Mineralisation at the Bogoso Gold Mine, Ghana, West Africa: Economic Geology, 97: 949-969.

Allibone, A., Hayden, P., Cameron, G. and Duku, F. (2004). Paleoproterozoic gold deposits hosted by albite- and carbonate-altered tonalite in the Chirano district, Ghana, West Africa: Economic Geology, 99: 479-497.

Beeson, J. (2011). Geological Model for the Paboase Gold deposit, Chirano Gold Mine, Ghana: Unpublished report prepared for Chirano Gold Mine Ltd. by Jigsaw Geoscience Pty Ltd. March 2011.

Ciftci, E., Kolayli, H. and Tokel, S. (2005). Lead- arsenic soil geochemical study as an exploration guide over the Killik volcanogenic massive sulphide deposit, northeastern Turkey: Journal of Geochemical Exploration, 86(1): 49-59.

Franklin, J. M. (1999). Systematic Analysis of Lithogeochemical Data, in Franklin, J.M., and Gibson, H.G., eds., Exploration Tools for Volcanogenic Massive Sulphide Deposits: Geological Association of Canada and Mineral Deposits Research Unit, U.B.C., Short Course Notes, Section 4

Gale, G. H., Fedikow, M. A. F. and Hutchinson, R. W. (2002). Distinguishing barren from productive exhalative strata and vectoring toward hydrothermal vent sites using Eu: Abstracts with Programs – Geological Society of America, 34(6): 113.

Halley, S. and Walshe, J. (2006). Alteration vectors to blind high-grade gold ore bodies: Bulletin – Australian Institute of Geoscientists, 44: 87-88.

Halley, S., (2011). Geochemistry of the Chirano Gold System: Unpublished report prepared for Chirano Gold Mine Ltd. by Mineral Mapping consulting April 2011.

Halley, S. (2009). Archean Gold Model: Unpublished report by Mineral Mapping consulting June, 2009.

Hirdes, W., Davis, D.W., and Eisenlohr, B.N. (1992). Reassessment of Proterozoic granitoid ages in Ghana on the basis of U/Pb zircon and monazite dating: Precambrian Research, 56: 89-96.

Leube, A., Hirdes, W., Mauer, R. and Kessie, G.O. (1990). The early Proterozoic Birimian Supergroup of Ghana and some aspects of its associated gold mineralisation. Precambrian Research 46: 139-165.

Jenner, G. A. (1996). Trace element geochemistry of igneous rocks: geochemical nomenclature and analytical geochemistry, in Wyman, D.A., ed., Trace Element Geochemistry of Volcanic Rocks: Applications for Massive Sulphide Exploration: Geological Association of Canada, Short Course Notes, 12: 51-77.

Micko, J. (2010). The geology, genesis and exploration context of the Central Zone alkali Cu-Au porphyry deposit, Galore Creek district, northwestern British Columbia, Canada, Vancouver, University of British Columbia, unpublished Ph.D thesis.

Neumayr, P., Walshe, J., Halley, S., Peterson, K., Pirlo, M., Young, C., Roache, A., Henson, P.A., Miller, J.M., William, N. and Blewett, R.S. (2006). Big system-big footprint; integrating Laverton's geology, geochemistry and geophysics for predictive mineral discovery: Record – Geoscience Australia, Report: 2006/07: 87-91.

Oberthür, T., Schmidt Mumm, A., Vetter, U., Simon, K. and Amanor, J.A. (1996). Gold mineralisation in the Ashanti Belt of Ghana: Genetic constraints of the stable isotope geochemistry: Economic Geology, 91: 259-301.

Oberthür, T., Vetter, U., Davis, D.W. and Amanor, J.A. (1998). Age constraints on gold mineralisation and Paleoproterozoic crustal evolution in the Ashanti belt of southern Ghana: Precambrian Research, 89: 129-143.

Prendergast, K. (2007). Application of lithogeochemistry to gold exploration in the St. Ives gold field, Western Australian. Geochemistry – Exploration, Environment, Analysis, 7(2): 99-108.

Roberts, J. M. (2010). Exploration on the Chirano Shear Zone using whole rock multi-element geochemistry, unpublished Master's Thesis.

Smeathers, C. (2009). Origins of mineralizing fluids in mesothermal shear zone-related mineralization of the Chirano gold district, Ghana, unpublished Master's thesis.

Spectral International Inc. (2005). Applied Reflectance Spectroscopy: Manual provided as an introduction to the process of collecting and interpreting data with ASD, version 4.1.

SRK, (2008). Chirano Structural Study: Unpublished report prepared for Red Back Mining Ghana Ltd. by SRK consulting May 2008.

Taylor, P. N., Moorbath, S., Leube, A. and Hirdes, W. (1992). Early Proterozoic crustal evolution in the Birimian of Ghana: Constraints from geochronology and isotope geochemistry: Precambrian Research, 56: 97-111.

Walshe, J., Neumayr, P. and Peterson, K. (2006). Scale-integrated, architectural and geodynamic controls on alteration and geochemistry of gold systems in the Eastern Goldfields Province, Yilgarn Craton; final report: Report – Minerals and Energy Research Institute of Western Australia, Report: 256, 290.

Yao, Y. and Robb, L.J. (2000). Gold mineralisation in Palaeoproterozoic granitoids at Obuasi, Ashanti region, Ghana: Ore geology, geochemistry and fluid characteristics: SouthAfrican Journal of Geology, 103: 255-278.

Yao, Y., Murphy, P.J. and Robb, L.J. (2001). Fluid characteristics of granitoid-hosted gold deposits in the Birimian Terrane of Ghana: A fluid inclusion microthermometric and Raman spectroscopic study: Economic Geology, 96: 1611-1643.